Supporting Information

Manipulating Clusters by Regulating N,O Chelating Ligands: Structures and Multistep Assembly Mechanisms

Hai-Ling Wang,[a,#] Zi-Yuan Liu,[a,#] Zhong-Hong Zhu,*[,a] Jin-Mei Peng,[a] Xiong-Feng Ma,*[,a] Juan Bai,[a] Hua-Hong Zou,*[,a] Kai-Qiang Mo,[a] and Fu-Pei Liang*[,a,b]

[a]State Key Laboratory for Chemistry and Molecular Engineering of Medicinal Resources, School of Chemistry & Pharmacy of Guangxi Normal University, Guilin 541004, P. R. China

[b]Guangxi Key Laboratory of Electrochemical and Magnetochemical Functional Materials, College of Chemistry and Bioengineering, Guilin University of Technology, Guilin 541004, P. R. China

Table of Contents:

Experimental

Materials and Measurements.

All reagents were obtained from commercial sources and used without further purification. Elemental analyses for C, H and N were performed on a vario MICRO cube. Thermogravimetric analyses (TGA) were conducted in a flow of nitrogen at a heating rate of 5 °C/min using a NETZSCH TG 209 F3 (Figure S1). Powder X-ray diffraction (PXRD) spectra were recorded on either a D8 Advance (Bruker) diffractometer at 293 K (Cu-Kα). The samples were prepared by crushing crystals and the powder placed on a grooved aluminum plate. Diffraction patterns were recorded from 5º to 60º at a rate of 5º min^{-1}. Calculated diffraction patterns of the compounds were generated with the Mercury software (Figure S2).Infrared spectra were recorded by transmission through KBr pellets containing *ca.* 0.5% of the complexes using a PE Spectrum FT-IR spectrometer (400-4,000 cm^{-1}).

Single-crystal X-ray crystallography.

Diffraction data for these complexes were collected on a Bruker SMART CCD diffractometer (Mo Kα radiation and λ = 0.71073 Å) in Φ and ω scan modes. The structures were solved by direct methods, followed by difference Fourier syntheses, and then refined by full-matrix least-squares techniques on F^2 using SHELXL.[1] All other non-hydrogen atoms were refined with anisotropic thermal parameters. Hydrogen atoms were placed at calculated positions and isotropically refined using a riding model. Table S3 summarizes X-ray crystallographic data and refinement details for the complexes. Full details can be found in the CIF files provided in the **Supporting Information**. The CCDC reference numbers are 1936731 (**1**), 1936732 (**2**) and 1936733 (**3**).

[1] Sheldrick, G. M. *Acta Crystallogr., Sect. C: Struct. Chem*. **2015**, *71*, 3-8.

HRESI-MS measurement.

HRESI-MS measurements were conducted at a capillary temperature of 275 °C. Aliquots of the solution were injected into the device at 0.3 mL/h. The mass spectrometer used for the measurements was a ThermoExactive, and the data were collected in positive and negative ion modes. The spectrometer was previously calibrated with the standard tune mix to give a precision of ca. 2 ppm within the region of 100−3,000 *m/z*. The capillary voltage was 50 V, the tube lens voltage was 150 V, and the skimmer voltage was 25 V.

Crystal structure determination.

For complex **2**, the voids are filled with disordered H_2O and CH_3OH molecules. The solvent-accessible volume is 334 $Å^3$ per unit cell volume. The diffraction data of compound was treated by the 'SQUEEZE' method as implemented in PLATON. SQUEEZE results for compound are as follows: SQUEEZE gives 94 electrons/unit cell for the voids, and each formula unit has 94/2 = 47 electrons (Z = 2). Each H_2O and each CH_3OH molecule has 10 and 18 electrons, respectively. Because of the disorder of the free CH_3OH and H_2O molecules, parts of the CH_3OH and H_2O molecules are difficult to locate in the final structural refinement. The number of free molecules is further confirmed by elemental analyses and TGA analysis. Therefore the chemical formula of complex is found to be $[Gd_9(\mathbf{L^2})_8(\mu_3\text{-OH})_8(\mu_4\text{-O})_2(NO_3)_8]\cdot 2CH_3OH\cdot H_2O$. For complex **3**, the voids are filled with disordered CH_3CN and CH_3OH molecules. The solvent-accessible volume is 3543.6 $Å^3$ per unit cell volume, and the pore volume ratio is 48.3% as calculated with the PLATON program. The diffraction data of compound was treated by the 'SQUEEZE' method as implemented in

PLATON. SQUEEZE results for compound are as follows: SQUEEZE gives 1926 electrons/unit cell for the voids, and each formula unit has 1926/2 = 963 electrons (Z = 2). Each CH_3CN and each CH_3OH molecule has 22 and 18 electrons, respectively. Because of the disorder of the free CH_3CN and CH_3OH molecules, parts of the CH_3CN and CH_3OH molecules are difficult to locate in the final structural refinement. The number of free molecules is further confirmed by elemental analyses and TGA analysis. Therefore the chemical formula of complex is found to be $[Gd_{12}(\mathbf{L^3})_8(OH)_{16}(NO_3)_8(OH)_4(H_2O)_4]\cdot 22CH_3OH\cdot 25CH_3CN$.

The synthesis of 1, 2 and 3.

Complex 1: A mixture of $Gd(NO_3)_3\cdot 6H_2O$ (0.2 mmol, 90.2 mg), H**L**^{1} ligand (1 mmol, 194 mg), triethylamine (10 μL), 1.2 mL mixted solvent (CH_3OH:CH_3CN = 3:1) were stirred and sealed in a 20 cm long Pyrex tube and heated at 80 °C for three days, then it was taken out and slowly cooled to room temperature. And faint yellow crystals were observed. The yield was about 30% (based on $Gd(NO_3)_3\cdot 6H_2O$). Anal. Calc. for $C_{20}H_{26}Gd_2N_8O_{16}$ (%): C, 25.31; H, 2.76; N, 11.81; Found: C, 25.15; H, 2.98; N, 11.52. IR (KBr, cm^{-1}): 3548 (w), 2895 (s), 2835 (s), 1643 (m), 1597 (m), 1483 (w), 1375 (w), 1305 (w), 1100 (m), 770 (s), 640 (s), 473 (s).

Complex 2: A mixture of $Gd(NO_3)_3\cdot 6H_2O$ (0.2 mmol, 90.2 mg), H**L**^{2} ligand (1 mmol, 105 mg), triethylamine (10 μL), 1.2 mL mixted solvent (CH_3OH:CH_3CN = 3:1) were stirred and sealed in a 20 cm long Pyrex tube and heated at 80 °C for three days, then it was taken out and slowly cooled to room temperature. And pellucid color crystals were observed. The yield was about 25% (based on $Gd(NO_3)_3\cdot 6H_2O$). Anal. Calc. for $C_{34}H_{90}Gd_9N_{16}O_{53}$ (%): C, 14.80; H, 3.01; N, 7.50; Found: C, 14.84; H, 3.11; N, 7.43. IR (KBr, cm^{-1}): 3518 (w), 2891 (s), 2832 (s), 1433 (w), 1372 (w), 1299 (w), 1106 (m), 768 (s), 636 (s), 474 (s).

Complex 3: A mixture of $Gd(NO_3)_3\cdot 6H_2O$ (0.2 mmol, 90.2 mg), H**L**^{3} ligand (1 mmol, 123 mg), triethylamine (10 μL), 1.2 mL mixted solvent (CH_3OH:CH_3CN = 3:1) were stirred and sealed in a 20 cm long Pyrex tube and heated at 80 °C for three days, then it was taken out and slowly cooled to room temperature. And pellucid color block crystals were observed. The yield was about 23% (based on $Gd(NO_3)_3\cdot 6H_2O$). Anal. Calc. for $C_{120}H_{195}Gd_{12}N_{41}O_{86}$ (%): C, 26.32; H, 3.56; N, 10.49; Found: C, 26.39; H, 3.58; N, 10.55. IR (KBr, cm^{-1}): 3533 (w), 2889 (s), 2831 (s), 1647 (m), 1590 (m), 1480 (w), 1379 (w), 1311 (w), 1108 (m), 773 (s), 641 (s), 478 (s).

Table S1. 43 examples of high-nuclear lanthanide clusters are known with nuclearity ≥10 was queried using Scifinder until 30 Aug. 2019. The number of genuine high-nuclear lanthanide clusters may be varied because of the term "high-nuclear lanthanide clusters" was not used in some papers.

No	Complexes	Ref.
1	$[Ln_{14}(CO_3)_{13}(ccnm)_9(OH)(H_2O)_6(phen)_{13}(NO_3)]\cdot(CO_3)_{2.5}\cdot(phen)_{0.5}$ (**Ln$_{14}$**)	1
2	$[Ln_{24}(DMC)_{36}(\mu_4\text{-}CO_3)_{18}(\mu_3\text{-}H_2O)_2]$ (**Ln$_{24}$**)	2, 3
3	$[(CO_3)_2@Ln_{37}(LH_3)_8(CH_3COO)_{21}(CO_3)_{12}(\mu_3\text{-}OH)_{41}(\mu_2\text{-}H_2O)_5(H_2O)_{40}]\cdot(ClO_4)_{21}\cdot 100(H_2O)$ (**Ln$_{37}$**)	4
4	$[Er_{60}(L\text{-thre})_{34}(\mu_6\text{-}CO_3)_8(\mu_3\text{-}OH)_{96}(\mu_2\text{-}O)_2(H_2O)_{18}]\cdot Br_{12}\cdot(ClO_4)_{18}\cdot 40(H_2O)$ (**Ln$_{60}$**)	5
5	$[Dy_{72}(mda)_{24}(mdaH)_8(OH)_{120}(O)_8(NO_3)_{16}]\cdot(NO_3)_8$ (**Ln$_{72}$**)	6
6	$[Gd_{38}(\mu\text{-}O)(\mu_8\text{-}ClO_4)_6(\mu_3\text{-}OH)_{42}(CAA)_{37}(H_2O)_{36}(EtOH)_6]\cdot(ClO_4)_{10}\cdot(OH)_{17}\cdot 14DMSO\cdot 13H_2O$ (**Ln$_{38}$**)	7
7	$[Gd_{48}(\mu_4\text{-}O)_6(\mu_3\text{-}OH)_{84}(CAA)_{36}(NO_3)_6(H_2O)_{24}(EtOH)_{12}(NO_3)Cl_2]\cdot Cl_3$ (**Ln$_{48}$**)	
8	$[Ln_{104}(ClO_4)_6(CH_3COO)_{56}(\mu_3\text{-}OH)_{168}(\mu_4\text{-}O)_{30}(H_2O)_{112}]\cdot(ClO_4)_{22}$ (**Ln$_{104}$**)	8

9	$\{[Ln_{36}(NA)_{36}(OH)_{49}(O)_6(NO_3)_6(N_3)_3(H_2O)_{20}]Cl_2\cdot 28H_2O\}_n$ (**Ln_{36}**)	9
10	$\{[Cl_2\&(NO_3)]@[Er_{48}(NA)_{44}(OH)_{90}(N_3)(H_2O)_{24}]\}_n$ (**Ln_{48}**)	10
11	$K_2[Ho_{48}(IN)_{46}(\mu_3\text{-}OH)_{84}(\mu_4\text{-}OH)_4(\mu_5\text{-}O)_2(OAc)_4(H_2O)_{14}(CO_3)Br_2]$ (**Ln_{48}**)	11
12	$[(ClO_4)@Ln_{27}(\mu_3\text{-}OH)_{32}(CO_3)_8(CH_3CH_2COO)_{20}(H_2O)_{40}]\cdot(ClO_4)_{12}\cdot(H_2O)_{50}$ (**Ln_{27}**)	12
13	$[Ln_{15}(\mu_3\text{-}OH)_{20}(\mu_5\text{-}X)]^{24+}$ (**Ln_{15}**)	13, 14
14	$[Dy_{19}(\mathbf{1}\text{-}3H)(\mathbf{1}\text{-}2H)_{11}(CH_3CO_2)_6(OH)_{26}(H_2O)_{30}]$ (**Ln_{19}**)	15
15	$Ln_{14}(\mu_4\text{-}OH)_2(\mu_3\text{-}OH)_{16}(\mu\text{-}\eta^2\text{-acac})_8(\eta^2\text{-acac})_{16}$ (**Ln_{14}**)	16
16	$H_{18}[Ln_{14}(\mu\text{-}\eta 2\text{-}O_2N\text{-}C_6H_4\text{-}O)_8(\eta 2\text{-}O_2N\text{-}C_6H_4\text{-}O)_{16}(\mu_4\text{-}O)_2(\mu_3\text{-}O)_{16}]$ (**Ln_{14}**)	17
17	$Ln_{14}(\mu_4\text{-}OH)_2(\mu_3\text{-}OH)_{16}(\mu\text{-}\eta^2\text{-acac})_8(\eta^2\text{-acac})_{16}\cdot 6H_2O$ (**Ln_{14}**)	18
18	$[Ho_{26}(IN)_{28}(CH_3COO)_4(CO_3)_{10}(OH)_{26}(H_2O)_{18}]\cdot 20H_2O$ (**Ln_{26}**)	19
19	$[Dy_{26}(\mu_3\text{-}OH)_{20}(\mu_3\text{-}O)_6(NO_3)_9I]^{36+}$ (**Ln_{26}**)	20
20	$[Gd_{10}(\mu_3\text{-}OH)_8]^{22+}$ (**Ln_{10}**)	21
21	$[Dy_{10}O_2(OH)_6(o\text{-van})_6(ISO)_{13}(H_2O)_2](NO_3)$ (**Ln_{10}**)	22
22	$[Ln_{10}(TBC8A)_2(PhPO_3)_4(OH)_2(HCO_3)(HCOO)(DMF)_{14}]\cdot(H_6TBC8A)\cdot 8CH_3OH$ (**Ln_{10}**)	23
23	$[Ln_{16}As_{16}W_{164}O_{576}(OH)_8(H_2O)_{42}]^{80-}$ (**Ln_{16}**)	24
24	$[Ln_{27}Ge_{10}W_{106}O_{406}(OH)_4(H_2O)_{24}]^{59-}$ (**Ln_{26}**)	25
25	$[Ln_{12}(L)_6(OH)_4O_2(CO_3)_6][Ln_{12}(L)_6(OH)_4O_4(CO_3)_6]\cdot(ClO_4)_4\cdot xH_2O$ (**Ln_{12}**)	26
26	$[Dy_{11}(OH)_{11}(phendox)_6(phenda)_3(OAc)_3]\cdot(OH)\cdot 40H_2O\cdot 7MeOH$ (**Ln_{11}**)	27
27	$[Gd_{60}(CO_3)_8(CH_3COO)_{12}(\mu_2\text{-}OH)_{24}(\mu_3\text{-}OH)_{96}(H_2O)_{56}](NO_3)_{15}\cdot Br_{12}\cdot(dmp)_5\cdot 30CH_3OH\cdot 20Hdmp$ (**Ln_{60}**)	28
28	$[Ln_{12}(fsa)_{12}(\mu f_3\text{-}OH)_{12}(DMF)_{12}]\cdot n DMF$ (**Ln_{12}**)	29
29	$(Pr_2NH_2)_5[Dy_{12}(OH)_{16}(SALO)_4(SALOH)_8(NO_3)_8(H_2O)_{0.5}]NO_3$ (**Ln_{12}**)	30
30	$[Dy_{12}(L)_8(OH)_{16}(CH_3O)_8(H_2O)_8]\cdot(CH_3O)_4$ (**Ln_{12}**)	31
31	$(H_3O)_6[Dy_{76}O_{10}(OH)_{138}(OAc)_{20}(L_1)_{44}(H_2O)_{34}]\cdot 2CO_3\cdot 4Cl\cdot 2L_1\cdot 2OAc$ (**Dy_{76}**)	32
32	$[Gd_{18}(ovpho)_6(OAc)_{30}(H2O)_6]\cdot 21CH_3OH\cdot 18H_2O$ (**Gd_{18}**)	33
33	$[Ln_{11}(ovpho)_4(\mu\text{-}CH_3O)_2(\mu\text{-}H_2O)_2(\mu_3\text{-}OH)_6(CH_3OH)_4(H_2O)_2(NO_3)_8](OH)\cdot xH_2O\cdot yCH_3OH$ (**Ln_{11}**)	34
34	$[Ln(\mu_3\text{-}OH)_8][Ln_{16}(\mu_4\text{-}O)(\mu_4\text{-}OH)(\mu_3\text{-}OH)_8(H_2O)_8(\mu_4\text{-}dcd)_8][(\mu_3\text{-}dcd)_8]\cdot 22H_2O$ (**Ln_{17}**)	35
35	$[Dy_{21}(L)_7(LH)_7(tfa)_7]\cdot Cl_7\cdot 15H_2O\cdot 7MeOH\cdot 12CHCl_3$ (**Ln_{21}**)	36
36	$Dy_{10}(MOE)_{30}$ (**Dy_{10}**)	37
37	$[Dy_{10}(\mu_3\text{-}OH)_4(OAc)_{20}(H_2L)_2(H_3L)_2\{NH_2C(CH_2OH)_3\}_2]$ (**Dy_{10}**)	38
38	$\{Dy_{12}(OH)_{16}(phenda)_8(H_2O)_8\}]^{2+}$ (**Dy_{12}**)	39
39	$[Dy_{14}(EDDC)_4(opch)_4(O_3PC_{10}H_7)_{10}(OAc)_6(H_2O)_4]\cdot xH_2O$ (**Dy_{14}**)	40
40	$[\{Dy_{15}(OH)_{20}(PepCO_2)_{10}(DBM)_{10}Cl\}Cl_4]$ (**Dy_{15}**)	41
41	$[Et_4N]_3[Ln_{16}(\mu_3\text{-}OH)_{24}(bsc)_6(H_2O)_{18}]Cl_{15}\cdot 2H_2O\cdot EtOH$ (**Dy_{16}**)	42
42	$[Dy_{20}(\mu_4\text{-}O)_{11}(\mu_3\text{-}OMe)_{12}(\mu\text{-}OMe)_8(MebptpO)_4(PhCO_2)_8(H_2O)_4](OH)_2\cdot xH_2O\cdot yMeOH\cdot zMeCN$ (**Dy_{20}**)	43
43	$\{Dy_5(EDDC)_2(\mu_3\text{-}AcO)_2(\mu_5\text{-}C_{15}H_{11}PO_3)(\mu_4\text{-}C_{15}H_{11}PO_3)(\mu_2\text{-}AcO)_2(AcO)_2(H_2O)\ (CH_3OH)_2\}_2(\mu_4\text{-}C_2O_4)\cdot xH_2O$ (**Dy_{10}**)	44

1. A.S. Chesman, D.R. Turner, B. Moubaraki, K.S. Murray, G.B. Deacon, S.R. Batten, *Dalton Trans*. **2012**, *41*, 10903–10909.
2. L.X. Chang, G. Xiong, L. Wang, P. Cheng, B. Zhao, *Chem. Commun*. **2013**, *49*, 1055–1057.

3. W. Li, G. Xiong, *Inorg.Chem. Commun*. **2015**, *59*, 1–4.
4. Y. Zhou, X.Y. Zheng, J. Cai, Z.F. Hong, Z.H. Yan, X.J. Kong, Y.P. Ren, L.S. Long, L.S.Zheng, *Inorg. Chem*. **2017**, *56*, 2037–2041.
5. X.-J. Kong, Y. Wu, L.-S. Long, L.-S. Zheng, Z. Zheng, *J. Am. Chem. Soc*. **2009**, *131*, 6918–6919.
6. L. Qin, Y.-Z. Yu, P.-Q. Liao, W. Xue, Z. Zheng, X.-M. Chen, Y.-Z. Zheng, *Adv. Mater.* **2016**, *28*, 10772–10779.
7. F.S. Guo, Y.C. Chen, L.L. Mao, W.Q. Lin, J.D. Leng, R. Tarasenko, M. Orendac, J.Prokleska, V. Sechovsky, M.L. Tong, *Chem.-Eur. J.* **2013**, *19*, 14786–14885.
8. J.-B. Peng, X.-J. Kong, Q.-C. Zhang, M. Orendac, J. Prokleska, Y.-P. Ren, L.-S. Long,Z. Zheng, L. Zheng, *J. Am. Chem. Soc*. **2014**, *136*, 17938–17941.
9. M. Wu, F. Jiang, X. Kong, D. Yuan, L. Long, S.A. Al-Thabaiti, M. Hong, *Chem. Sci*. **2013**, *4*, 3104–3109.
10. M. Wu, F. Jiang, D. Yuan, J. Pang, J. Qian, S.A. Al-Thabaiti, M. Hong, *Chem. Commun*. **2014**,*50*, 1113–1115.
11. L. Chen, J.Y. Guo, X. Xu, W.W. Ju, D. Zhang, D.R. Zhu, Y. Xu, *Chem. Commun*. **2013**, *49*, 9728–9730.
12. X.-Y. Zheng, J.-B. Peng, X.-J. Kong, L.-S. Long, L.-S. Zheng, *Inorg. Chem. Front*. **2016**, *3*, 320–325.
13. R. Wang, Z. Zheng, T. Jin, R.J. Staples, *Angew. Chem. Int. Ed*. **1999**, *38*, 1813–1815.
14. R. Wang, H.D. Selby, H. Liu, M.D. Carducci, T. Jin, Z. Zheng, J.W. Anthis, R.J.Staples, *Inorg. Chem*. **2002**, *41*, 278–286.
15. D. D'Alessio, A.N. Sobolev, B.W. Skelton, R.O. Fuller, R.C. Woodward, N.A.Lengkeek, B.H. Fraser, M. Massi, M.I. Ogden, *J. Am. Chem. Soc*. **2014**, *136*, 15122–15125.
16. R. Wang, D. Song, S. Wang, *Chem. Commun*. **2002**, 368–369.
17. M.R. Bürgstein, M.T. Gamer, P.W. Roesky, *J. Am. Chem. Soc*. **2004**, *126*, 5213–5218.
18. X.-L. Li, L.-F. He, X.-L. Feng, Y. Song, M. Hu, L.-F. Han, X.-J. Zheng, Z.-H. Zhang, S.-M. Fang, *CrystEngComm*, **2011**, *13*, 3643–3645.
19. L. Chen, L. Huang, C. Wang, J. Fu, D. Zhang, D. Zhu, Y. Xu, *J. Coord. Chem*. **2012**, *65*, 958–968.
20. X. Gu, D. Xue, *Inorg. Chem*. **2007**, *46*, 3212–3216.
21. S.J. Liu, J.P. Zhao, J. Tao, J.M. Jia, S.D. Han, Y. Li, Y.C. Chen, X.H. Bu, *Inorg. Chem*. **2013**, *52*, 9163–9165.
22. S.K. Langley, B. Moubaraki, K.S. Murray, *Polyhedron*, **2013**, *64*, 255–261.
23. K. Su, F. Jiang, J. Qian, J. Pang, F. Hu, S.M. Bawaked, M. Mokhtar, S.A. Al-Thabaiti,M. Hong, *Inorg. Chem. Commun*. **2015**,*54*, 34–37.
24. F. Hussain, G.R. Patzke, *CrystEngComm*, **2011**, *13*, 530–536.
25. Z. Li, X.X. Li, T. Yang, Z.W. Cai, S.T. Zheng, *Angew. Chem. Int. Ed*. **2017**, *56*, 2664–2669.
26. L. Zhao, S. Xue, J. Tang, *Inorg. Chem.* **2012**, *51*, 5994–5996.
27. Y.L. Miao, J.L. Liu, J.Y. Li, J.D. Leng, Y.C. Ou, M.L. Tong, *Dalton Trans*. **2011**, *40*, 10229–10236.
28. X.-M. Luo, Z.-B. Hu, Q.-F. Lin, W. Cheng, J.-P. Cao, C.-H. Cui, H. Mei, Y. Song, Y. Xu, *J. Am. Chem. Soc.*, **2018**, *140*, 11219–11222
29. A. S. Dinca, A. Mindru, D. Dragancea, C. Tiseanu, S. Shova, S. Cornia, L. M. Carrella, E. Rentschler, M. Affronte, M. Andruh, *Dalton Trans*. **2019**, *48*, 1700–1708.
30. L. R. Piquer, M. Escoda-Torroella, M. L. Gairaud, S. Carneros, N. Daffé, M. Studniarek, J. Dreiser, W. Wernsdorfer, E. C. Sañudo, *Inorg. Chem. Front*. **2019**, *6*, 705–714.

31. X.-F. Ma, H.-L. Wang, Z.-H. Zhu, B. Li, K.-Q. Mo, H.-H. Zou, F.-P. Liang, *Dalton Trans*. DOI: 10.1039/C9DT01454C.
32. X.-Y. Li, H.-F. Su, Q.-W. Li, R. Feng, H.-Y. Bai, H.-Y. Chen, J. Xu, X.-H. Bu, *Angew. Chem. Int. Ed.* **2019**, *58*, 10184–10188.
33. K. Wang, Z. L. Chen, H. H. Zou, K. Hu, H. Y. Li, Z. Zhang, W. Y. Sun, F. P. Liang, *Chem. Commun.* **2016**, *52*, 8297–8300.
34. K. Wang, Z. L. Chen, H. H. Zou, S. H. Zhang, Y. Li, X. Q. Zhang, W. Y. Sun, F. P. Liang, *Dalt. Trans.* **2018**, *47*, 2337–2343.
35. Y.-Y. Zhou, B. Geng, Z.-W. Zhang, Q. Guan, J.-L. Lu, Q.-B. Bo, *Inorg. Chem.*, **2016**, *55*, 2037−2047.
36. S. Biswas, S. Das, J. Acharya, V. Kumar, J. Leusen, P. Kögerler, J. M. Herrera, E. Colacio, V. Chandrasekhar, *Chem. Eur. J.* **2017**, *23*, 5154–5170.
37. L. G. Westin, M. Kritikos, A. Caneschi, *Chem. Commun.* **2003**, 1012–1013.
38. H. Ke, G.-F. Xu, L. Zhao, J. Tang, X.-Y. Zhang, H.-J. Zhang, *Chem. Eur. J.* **2009**, *15*, 10335–10338.
39. Y.-L. Miao, J.-L. Liu, J.-D. Leng, Z.-J. Lin, M.-L. Tong, *CrystEngComm.* **2011**, *13*, 3345–3348.
40. H. Tian, S.-S. Bao, L.-M. Zheng, *Chem. Commun.* **2016**, *52*, 2314-2317.
41. D. T. Thielemann, A. T. Wagner, Y. Lan, P. Oña-Burgos, I. Fernández, E. S. Rösch, D. K. Kölmel, A. K. Powell, S. Bräse, P. W. Roesky, *Chem. Eur. J.* **2015**, *21*, 2813–2820.
42. P. Richardson, T.-J. Hsu, C.-J. Kuo, R. J. Holmberg, B. Gabidullin, M. Rouzières, R. Clérac, M. Murugesu, P.-H. Lin, *Dalton Trans.* **2018**, *47*, 12847–12851.
43. W.-Q. Lin, X.-F. Liao, J.-H. Jia, J.-D. Leng, J.-L. Liu, F.-S. Guo, M.-L. Tong, *Chem. Eur. J.* **2013**, *19*, 12254–12258.
44. H. Tian, J.-B. Su, S.-S. Bao, M. Kurmoo, X.-D. Huang, Y.-Q. Zhang, L.-M. Zheng, *Chem. Sci.* **2018**, *9*, 6424–6433.

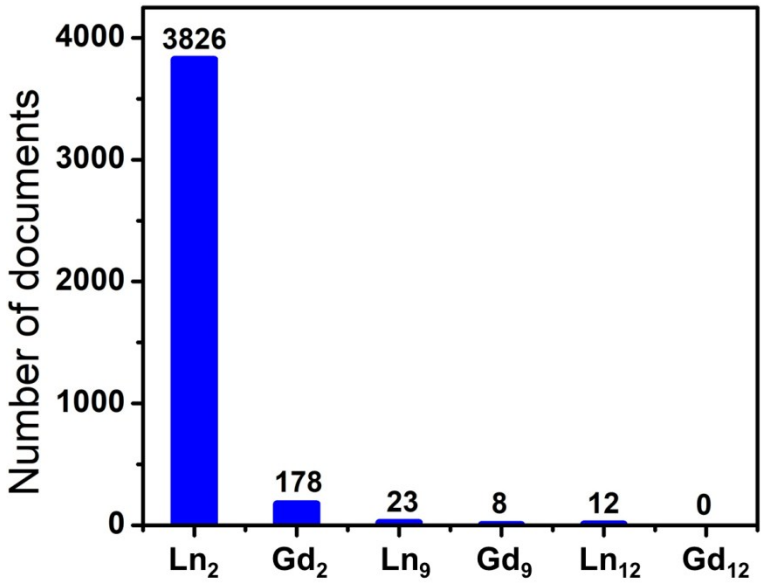

Scheme S1. The different structure containing dimer Ln_2 and Gd_2, "hourglass-like" enneanuclear Ln_9 and Gd_9, vertex-sharing $\{M_4O_4\}$ cubanes Ln_{12} and Gd_{12} was counted using CCDC2019 (2.0.2) until 30 Aug. 2019.

Table S2a. The M_9 structure containing "hourglass-like" enneanuclear complexes was queried using CCDC2019 (2.0.2) until 30 Aug. 2019.

No	Title	Structure	Ref.
1	A novel example of self-assembly in lanthanide chemistry: synthesis and molecular structure of $[Na(EtOH)_6][Y_9(\mu_4\text{-}O)_2(\mu_3\text{-}OH)_8\{\mu\text{-}\eta^2\text{-}MeC(O)CHC(O)OEt\}_8\{\eta^2\text{-}MeC(O)CHC(O)OEt\}_8]$	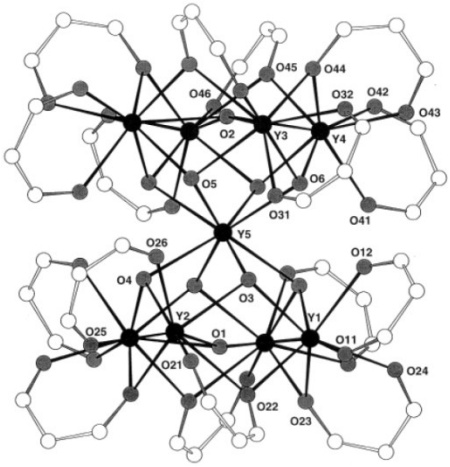	*J. Chem. Soc., Dalton Trans.*, **1999**, 4127–4130
2	Synthesis and Structural Characterization of Nonanuclear Lanthanide Complexes	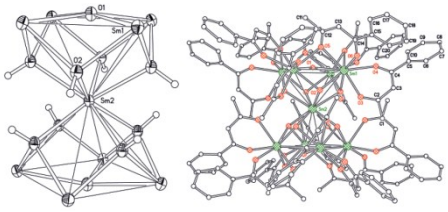	*Inorg. Chem.* **2002**, *41*, 6802-6807
3	Synthesis and physico-chemical characterization of a new series of hydroxide ion acetylacetonate lanthanide(III)—ditungsten decacarbonyl hydride complexes	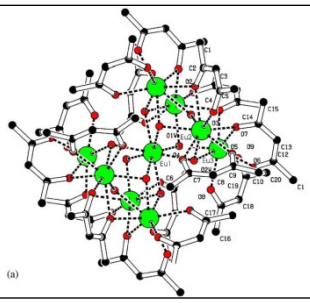	*J. Alloy Compd.* **2004**, *374*, 382–386
4	Assembling Process of Charged Nonanuclear Cationic Lanthanide(III) Clusters Assisted by Dichromium Decacarbonyl Hydride	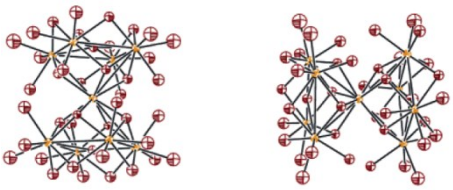	*Inorg. Chem.* **2004**, *43*, 1603-1605
5	Synthesis and X-ray crystal structure of cationic polynuclear hydroxide acetylacetonate lanthanide(III) clusters with homodinuclear or heterodinuclear decacarbonyl hydrides: $[HMo_2(CO)_{10}]^-$ and $[HCrW(CO)_{10}]^-$	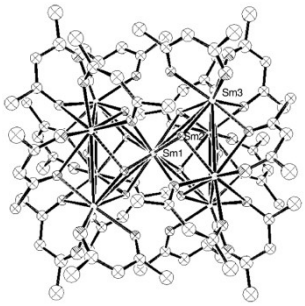	*J. Alloy Compd.* **2006**, *408–412*, 1046–1051

6	Effective and efficient photoluminescence of salicylate-ligating terbium(III) clusters stabilized by multiple phenyl–phenyl interactions	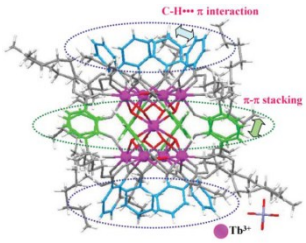	*Chem. Commun.*, **2007**, 1242–1244
7	Crystal structure and photo- and electroluminescent properties of a ‘‘sandglass” terbium cluster	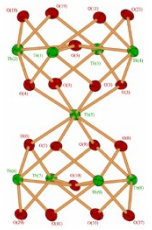	*Inorg. Chem. Commun.* **2008**, *11*, 1187–1189
8	Luminescence spectroscopy of europium(III) and terbium(III) penta-, octa- and nonanuclear clusters with b-diketonate ligands	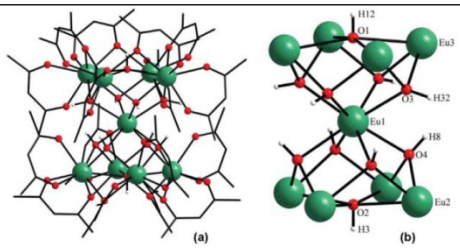	*Dalton Trans.*, **2009**, 6809–6815
9	Praseodymium(III)-based bis-metallacalix[4]arene with host–guest behaviour	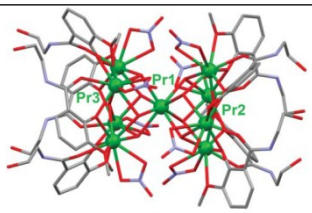	*Dalton Trans.*, **2010**, *39*, 4353–4357
10	Hydrolytic synthesis and structural characterization of lanthanide-acetylacetonato/hydroxo cluster complexes – A systematic study	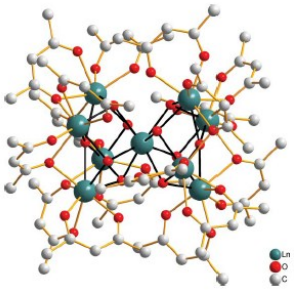	*Dalton Trans.*, **2011**, *40*, 1041–1046
11	A diabolo-shaped Dy9 cluster: synthesis, crystal structure and magnetic properties	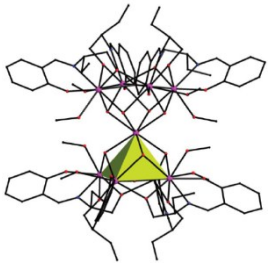	*Dalton Trans.*, **2011**, *40*, 6440–6444
12	Systematic study of the formation of the lanthanoid cubane cluster motif mediated by steric modification of diketonate ligands	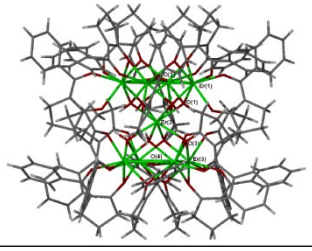	*Dalton Trans.*, **2011**, *40*, 12169–12179

13	A New Family of Nonanuclear Lanthanide Clusters Displaying Magnetic and Optical Properties	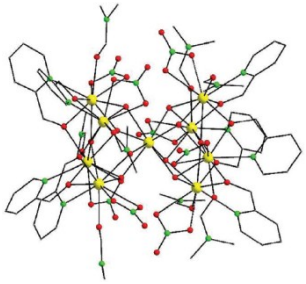	*Inorg. Chem*. **2011**, *50*, 11276−11278
14	Nonanuclear lanthanide(III) nanoclusters: Structure, luminescence and magnetic properties	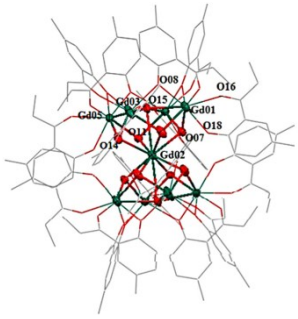	*Polyhedron* **2013**, *53*, 187–192
15	Systematic Study of the Luminescent Europium-Based Nonanuclear Clusters with Modified 2-Hydroxybenzophenone Ligands	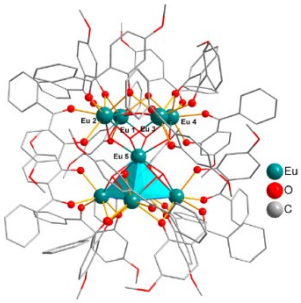	*Inorg. Chem*. **2013**, *52*, 13332−13340
16	Enhancement of Optical Faraday Effect of Nonanuclear Tb(III) Complexes	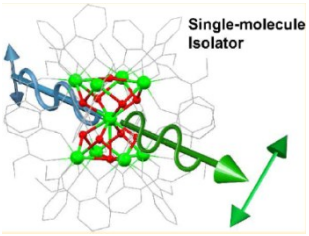	*Inorg. Chem*. **2014**, *53*, 7635−7641
17	Lanthanide nonanuclear clusters with sandglass-like topology and the SMM behavior of dysprosium analogue	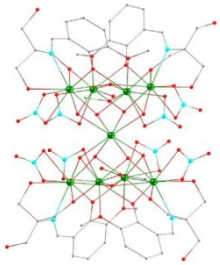	*Polyhedron* **2015**, *88*, 110–115
18	Redox shield enfolding a magnetic core	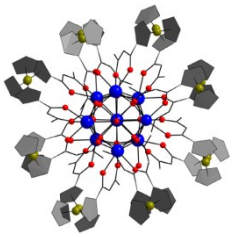	*Polyhedron* **2015**, *102*, 361–365

19	Critical Role of Energy Transfer Between Terbium Ions for Suppression of Back Energy Transfer in Nonanuclear Terbium Clusters	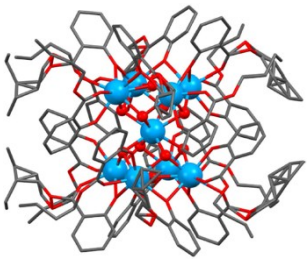	*Sci. Rep.* **2016**, *6*, 37008
20	A stable nonanuclear Tb(III) cluster for selective sensing of picric acid	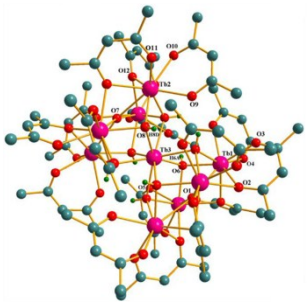	*Inorg. Chim. Acta*. **2017**, *463*, 14–19
21	2-hydroxybenzophenone-controlled self-assembly of enneanuclear lanthanide(III) hydroxo coordination clusters with an "hourglass"-like topology	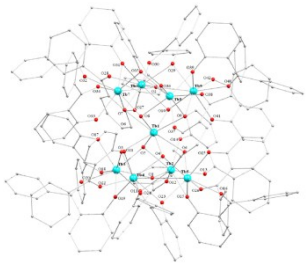	*Inorg. Chem. Commun*. **2017**, *83*, 118–122
22	Topological Self-Assembly of Highly Symmetric Lanthanide Clusters: A Magnetic Study of Exchange-Coupling "Fingerprints" in Giant Gadolinium(III) Cages	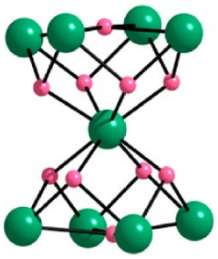	*J. Am. Chem. Soc*. **2017**, *139*, 16405–16411
23	Syntheses, crystal structures and magnetic properties of sandglass Dy^{III}_9 and irregular tetrahedron Dy^{III}_4 complexes	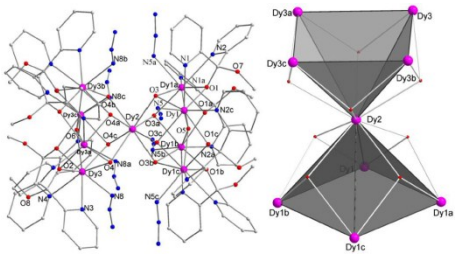	*Polyhedron* **2018**, *141*, 69–76
24	Two New Series of Potentially Triboluminescent Lanthanide(III) *β*-Diketonate Complexes	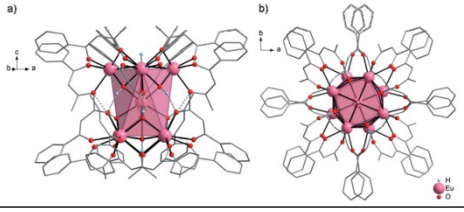	*Z. Anorg. Allg. Chem*. **2018**, 1177–1184

Table S2b. The M_{12} structure containing Vertex-Sharing $\{M_4O_4\}$ Cubanes was queried using CCDC2018 (2.00) until 30 Aug. 2019.

No	Title	Structure	Ref.
1	Chloride templated formation of$\{Dy_{12}(OH)_{16}\}^{20+}$ cluster core incorporating1,10-phenanthroline-2,9-dicarboxylate	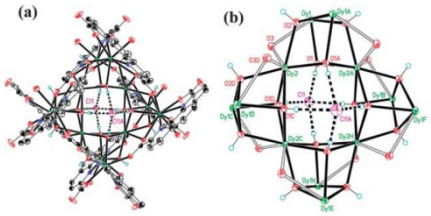	*CrystEngComm*, **2011**, *13*, 3345–3348.
2	The Importance of Being Exchanged: $[Gd^{III}_4M^{II}_8(OH)_8(L)_8(O_2CR)_8]^{4+}$Clusters for MagneticRefrigeration	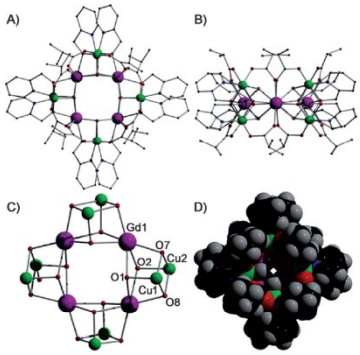	*Angew. Chem. Int. Ed.* **2012**, *51*, 4633 –4636.
3	Chiral biomolecule based dodecanucleardysprosium(III)–copper(II)clusters: structuralanalyses and magnetic properties	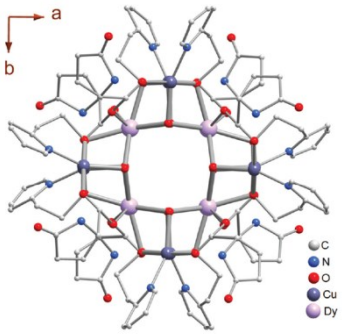	*Inorg. Chem. Front.* **2015**, *2*, 854–859.
4	$Cu^{II}Gd^{III}$ Cryogenic Magnetic Refrigerants and Cu_8Dy_9 Single-MoleculeMagnet Generated by In Situ Reactions of Picolinaldehyde and Acetylpyridine: Experimental and Theoretical Study	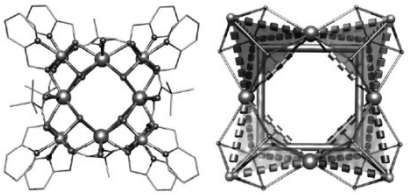	*Chem. Eur. J.* **2013**, *19*, 17567–17577.
5	Structurally Flexible and Solution Stable$[Ln_4TM_8(OH)_8(L)_8(O_2CR)_8(MeOH)_y](ClO_4)_4$: A Play ground for Magnetic Refrigeration	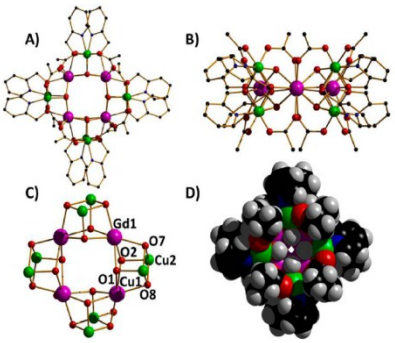	*Inorg. Chem.* **2016**, *55*, 10535−10546.

6	Filling the Missing Links of M_{3n} Prototype 3d-4f and 4f Cyclic Coordination Cages: Syntheses, Structures, and Magnetic Properties of the $Ni_{10}Ln_5$ and the Er_{3n}Wheels	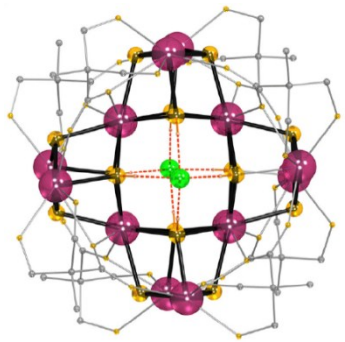	*Inorg. Chem.* **2017**, *56*, 12821−12829.
7	Halide-Templated Assembly of Polynuclear Lanthanide-Hydroxo Complexes	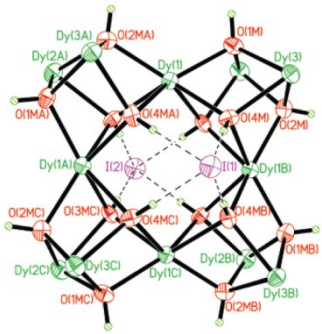	*Inorg. Chem.* **2002**, *41*, 278-286.
8	Synthesis, Structure, and Magnetism of a Family of Heterometallic$\{Cu_2Ln_7\}$ and $\{Cu_4Ln_{12}\}$ (Ln = Gd, Tb, and Dy) Complexes: The Gd Analogues Exhibiting a Large Magnetocaloric Effect	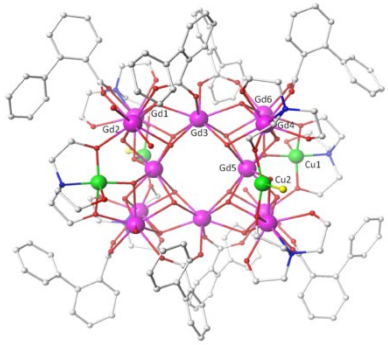	*Inorg. Chem.* **2014**, *53*,13154−13161.
9	Benzoxazole-Based Heterometallic Dodecanuclear Complex $[Dy^{III}_4Cu^{II}_8]$ with Single-Molecule-Magnet Behavior	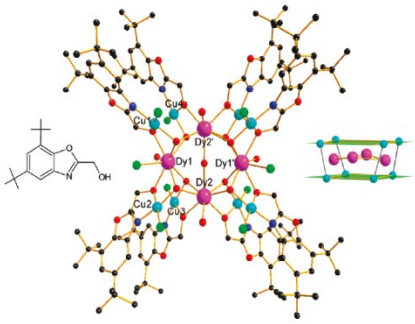	*Inorg. Chem.* **2011**, *50,* 7373–7375

10	Hysteresis enhancement on a hybrid Dy(III) single molecule magnet/iron oxide nanoparticle system	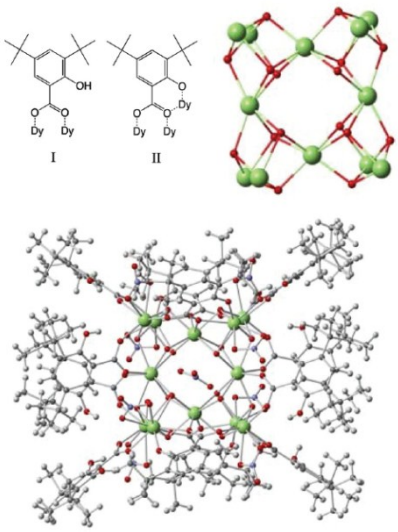	*Inorg. Chem. Front.*, **2019**, *6*, 705–714
11	Aggregation of $[Ln^{III}_{12}]$ clusters by the dianion of 3-formylsalicylic acid. Synthesis, crystal structures, magnetic and luminescence properties	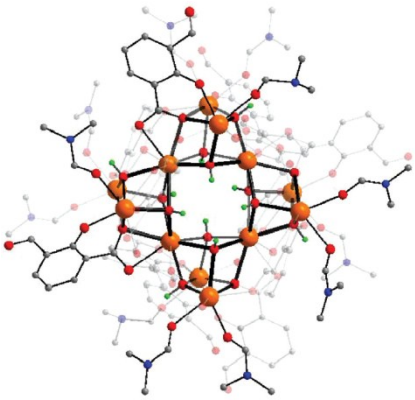	*Dalton Trans.*, **2019**, *48*, 1700–1708
12	Formation of nanocluster $\{Dy_{12}\}$ containing Dy-exclusive vertex-sharing $[Dy_4(\mu_3\text{-OH})_4]$ cubanes via simultaneous multitemplate guided and step-by-step assembly	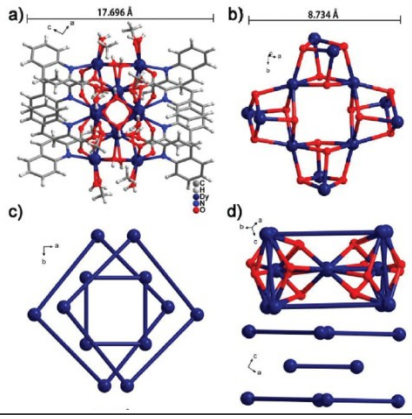	*Dalton Trans.*, **2019**, *48*, 11338-11344.

Table S3. Crystallographic data of the complexes **1**, **2** and **3**.

Complex	**1**	**2**	**3**
Formula	$C_{20}H_{26}Gd_2N_8O_{16}$	$C_{34}H_{90}Gd_9N_{16}O_{53}$	$C_{120}H_{195}Gd_{12}N_{41}O_{86}$
Formula weight	948.99	2985.25	5472.00
T (K)	293 (2)	293 (2)	296.15
Crystal system	Triclinic	Tetragonal	Tetragonal
Space group	$P\bar{1}$	*P*4*nc*	*I*422

a (Å)	8.3885 (4)	17.3000 (2)	18.4916 (16)
b (Å)	8.5010 (4)	17.3000 (2)	18.4916 (16)
c (Å)	12.0706 (6)	14.4460 (3)	21.4412 (19)
α (°)	106.9550 (10)	90.00	90.00
β (°)	105.9010 (10)	90.00	90.00
γ (°)	100.7070 (10)	90.00	90.00
V (Å^3)	758.10 (6)	4323.57	7331.6 (11)
Z	1	2	2
D_c(g cm^{-3})	2.079	2.231	1.696
μ (mm^{-1})	4.422	6.895	5.417
Reflns coll.	12735	16198	16595
Unique reflns	3483	3895	4218
R_{int}	0.0293	0.0275	0.0431
$^aR_1[I \geq 2\sigma(I)]$	0.0281	0.0239	0.0535
$^bwR_2$(all data)	0.0973	0.0618	0.1624
GOF	1.162	1.103	1.075

$^aR_1 = \Sigma||F_o|-|F_c||/\Sigma|F_o|$, $^bwR_2 = [\Sigma w(F_o^2-F_c^2)^2/\Sigma w(F_o^2)^2]^{1/2}$

Table S4. Selected bond lengths (Å) and angles (°) of complexes **1**, **2** and **3**.

1					
Bond lengths (Å)					
Gd1—O3	2.507 (3)	Gd1—O1	2.477 (3)	Gd1—O2^i	2.274 (3)
Gd1—O6	2.465 (3)	Gd1—O4	2.529 (3)	Gd1—N1	2.642 (3)
Gd1—O7	2.498 (3)	Gd1—O2	2.278 (3)	Gd1—N2	2.534 (3)
Bond angles (°)					
O3—Gd1—O4	50.4 (1)	O7—Gd1—N2	78.3 (1)	O2^i—Gd1—O7	77.4 (1)
O3—Gd1—N1	73.9 (1)	O1—Gd1—O3	74.08 (1)	O2—Gd1—O7	129.4 (1)
O3—Gd1—N2	72.0 (1)	O1—Gd1—O7	115.5 (1)	O2^i—Gd1—O1	133.83 (9)
O6—Gd1—O3	143.2 (1)	O1—Gd1—O4	117.6 (1)	O2—Gd1—O1	67.69 (9)
O6—Gd1—O7	50.8 (1)	O1—Gd1—N1	124.6 (1)	O2^i—Gd1—O4	76.6 (1)
O6—Gd1—O1	72.0 (1)	O1—Gd1—N2	64.4 (1)	O2—Gd1—O4	84.6 (1)

O6—Gd1—O4	165.5 (1)	O4—Gd1—N1	69.5 (1)	O2^{i}—Gd1—O2	70.7 (1)
O6—Gd1—N1	115.3 (1)	O4—Gd1—N2	112.8 (1)	O2^{i}—Gd1—N1	101.6 (1)
O6—Gd1—N2	80.9 (1)	O2^{i}—Gd1—O3	125.4 (1)	O2—Gd1—N1	154.0 (1)
O7—Gd1—O3	140.4 (1)	O2—Gd1—O3	90.2 (1)	O2^{i}—Gd1—N2	154.8 (1)
O7—Gd1—O4	124.9 (1)	O2^{i}—Gd1—O6	89.0 (1)	O2—Gd1—N2	131.8 (1)
O7—Gd1—N1	69.5 (1)	O2—Gd1—O6	89.8 (1)	N2—Gd1—N1	63.2 (1)
Gd1^{i}—O2—Gd1	109.3 (1)				
Symmetry code: (i) -*x*, -*y*, -*z*.					
2					
Bond lengths (Å)					
Gd1—O1	2.477 (5)	Gd1—N1	2.570 (5)	Gd3—O10	2.321 (5)
Gd1—O2	2.307 (4)	Gd2—O4	2.437 (4)	Gd3—O10^{ii}	2.329 (5)
Gd1—O3	2.5367 (8)	Gd2—O8	2.434 (4)	Gd3—O11	2.500 (6)
Gd1—O4^{i}	2.399 (4)	Gd3—O8^{i}	2.375 (4)	Gd3—O12	2.620 (6)
Gd1—O4	2.320 (4)	Gd3—O8	2.351 (4)	Gd3—O13	2.530 (5)
Gd1—O5	2.553 (5)	Gd3—O9	2.5584 (9)	Gd3—N3	2.573 (7)
Gd1—O6	2.590 (5)				
Bond angles (°)					
O1—Gd1—O3	120.0 (2)	O4^{i}—Gd1—N1	140.5 (2)	O10^{ii}—Gd3—O9	67.3 (2)
O1—Gd1—O5	72.7 (2)	O5—Gd1—O6	49.1 (2)	O10—Gd3—O10^{ii}	98.4 (3)
O1—Gd1—O6	110.0 (2)	O5—Gd1—N1	81.3 (2)	O10^{ii}—Gd3—O11	81.3 (2)
O1—Gd1—N1	66.3 (2)	N1—Gd1—O6	69.3 (2)	O10—Gd3—O11	67.1 (2)
O2^{ii}—Gd1—O1	78.8 (2)	O4^{i}—Gd2—O4	72.7 (1)	O10—Gd3—O12	128.5 (2)
O2—Gd1—O1	68.6 (2)	O4^{iii}—Gd2—O4	113.9 (2)	O10^{ii}—Gd3—O12	132.8 (2)
O2—Gd1—O2^{ii}	96.8 (2)	O8^{ii}—Gd2—O4^{i}	138.4 (1)	O10^{ii}—Gd3—O13	151.3 (2)
O2—Gd1—O3	68.1 (2)	O8^{i}—Gd2—O4	146.7 (1)	O10—Gd3—O13	84.5 (2)
O2^{ii}—Gd1—O3	67.4 (2)	O8—Gd2—O4^{iii}	138.4 (1)	O10—Gd3—N3	131.8 (2)
O2^{ii}—Gd1—O4^{i}	131.3 (1)	O8—Gd2—O4	81.1 (1)	O10^{ii}—Gd3—N3	78.3 (2)
O2—Gd1—O4	132.8 (1)	O8—Gd2—O4^{i}	75.9 (2)	O11—Gd3—O9	118.8 (3)
O2—Gd1—O4^{i}	75.4 (2)	O8^{i}—Gd2—O8^{ii}	114.2 (2)	O11—Gd3—O12	110.4 (2)
O2^{ii}—Gd1—O5	149.6 (2)	O8—Gd2—O8^{i}	72.8 (1)	O11—Gd3—O13	73.6 (2)
O2—Gd1—O5	82.9 (2)	O8—Gd2—O8^{iii}	114.2 (2)	O11—Gd3—N3	64.9 (2)
O2^{ii}—Gd1—O6	137.2 (2)	O8—Gd3—O8^{i}	75.4 (2)	O13—Gd3—O9	137.7 (1)

O2—Gd1—O6	125.7 (2)	O8—Gd3—O9	65.7 (2)	O13—Gd3—O12	49.4 (2)
O2^{ii}—Gd1—N1	77.4 (2)	O8^{i}—Gd3—O9	65.4 (2)	O13—Gd3—N3	78.7 (2)
O2—Gd1—N1	134.8 (2)	O8—Gd3—O11	151.2 (2)	N3—Gd3—O12	67.6 (2)
O3—Gd1—O5	137.6 (2)	O8^{i}—Gd3—O11	133.2 (2)	Gd1—O2—Gd1^{i}	100.4 (2)
O3—Gd1—O6	128.8 (2)	O8—Gd3—O12	76.4 (2)	Gd1—O3—Gd1^{i}	89.70 (3)
O3—Gd1—N1	141.0 (1)	O8^{i}—Gd3—O12	74.2 (2)	Gd1—O3—Gd1^{iii}	171.7 (4)
O4—Gd1—O1	148.6 (2)	O8^{i}—Gd3—O13	77.3 (2)	Gd1—O3—Gd1^{ii}	89.70 (3)
O4^{i}—Gd1—O1	135.8 (2)	O8—Gd3—O13	124.1 (2)	Gd1—O4—Gd1^{ii}	98.6 (2)
O4—Gd1—O2^{ii}	76.1 (2)	O8—Gd3—N3	94.5 (2)	Gd1^{ii}—O4—Gd2	103.9 (1)
O4—Gd1—O3	66.2 (2)	O8^{i}—Gd3—N3	141.8 (2)	Gd1—O4—Gd2	106.3 (1)
O4^{i}—Gd1—O3	65.1 (2)	O9—Gd3—O12	129.8 (3)	Gd3^{ii}—O8—Gd2	104.8 (2)
O4—Gd1—O4^{i}	75.5 (2)	O9—Gd3—N3	143.5 (2)	Gd3—O8—Gd2	105.5 (2)
O4^{i}—Gd1—O5	78.3 (2)	O10^{ii}—Gd3—O8^{i}	131.2 (2)	Gd3—O8—Gd3^{ii}	99.7 (2)
O4—Gd1—O5	125.7 (2)	O10—Gd3—O8^{i}	74.4 (2)	Gd3—O9—Gd3^{iii}	170.6 (5)
O4—Gd1—O6	77.5 (2)	O10^{ii}—Gd3—O8	74.8 (2)	Gd3—O9—Gd3^{i}	89.61 (4)
O4^{i}—Gd1—O6	71.8 (2)	O10—Gd3—O8	131.5 (2)	Gd3—O10—Gd3^{i}	101.7 (2)
O4—Gd1—N1	89.9 (2)	O10—Gd3—O9	67.5 (2)		
Symmetry codes: (i) *y*, -*x*+1, *z*; (ii) -*y*+1, *x*, *z*; (iii) -*x*+1, -*y*+1, *z*.					
3					
Bond lengths (Å)					
Gd1—O7^{ii}	2.394 (8)	Gd1—O8^{ii}	2.391 (6)	Gd2—O1^{ii}	2.409 (7)
Gd1—O7	2.400 (8)	Gd1—O6	2.424 (9)	Gd2—O8^{ii}	2.394 (6)
Gd1—O1^{iii}	2.529 (7)	Gd1—O3	2.560 (9)	Gd2—O8	2.347 (7)
Gd1—O2	2.385 (8)	Gd2—O7	2.312 (8)	N1—Gd1^{i}	2.610 (12)
Bond angles (°)					
O7^{ii}—Gd1—O7	68.0 (4)	O2—Gd1—N1^{iii}	75.2 (5)	O7—Gd2—O8^{ii}	75.9 (3)
O7^{ii}—Gd1—O1^{iii}	121.9 (3)	O2—Gd1—O4	93.7 (4)	O7—Gd2—O8	70.6 (3)
O7—Gd1—O1^{iii}	67.3 (3)	O8^{ii}—Gd1—O7	74.0 (3)	O7—Gd2—O8^{iii}	140.0 (3)
O7^{ii}—Gd1—O8^{ii}	68.1 (3)	O8^{ii}—Gd1—O1^{iii}	65.3 (3)	O1^{iii}—Gd2—O1^{ii}	126.4 (5)
O7^{ii}—Gd1—O6	128.3 (4)	O8^{ii}—Gd1—O6	139.6 (4)	O8—Gd2—O1^{iii}	127.8 (3)
O7—Gd1—O6	79.9 (4)	O8^{ii}—Gd1—O3	143.7 (4)	O8^{ii}—Gd2—O1^{iii}	67.4 (3)
O7^{ii}—Gd1—O3	107.5 (4)	O8^{ii}—Gd1—N1^{iii}	93.4 (4)	O8—Gd2—O1^{ii}	81.5 (3)

O7—Gd1—O3	139.9 (4)	O8^{ii}—Gd1—O4	138.2 (4)	O8^{ii}—Gd2—O1^{ii}	148.9 (3)
O7^{ii}—Gd1—N1^{iii}	151.9 (5)	O6—Gd1—O1^{iii}	76.5 (4)	O8^{iii}—Gd2—O8^{ii}	116.9 (4)
O7—Gd1—N1^{iii}	128.8 (4)	O6—Gd1—O3	72.8 (5)	O8—Gd2—O8^{ii}	70.1 (3)
O7^{ii}—Gd1—O4	70.3 (4)	O6—Gd1—N1^{iii}	79.5 (5)	O8—Gd2—O8^{iii}	78.5 (4)
O7—Gd1—O4	94.5 (4)	O6—Gd1—O4	73.2 (5)	O8^{iv}—Gd2—O8	117.9 (4)
O1^{iii}—Gd1—O3	130.6 (4)	O3—Gd1—N1^{iii}	74.5 (4)	Gd1^{ii}—O7—Gd1	110.4 (4)
O1^{iii}—Gd1—N1^{iii}	62.5 (4)	O4—Gd1—O1^{iii}	146.9 (4)	Gd2—O7—Gd1	99.0 (4)
O2—Gd1—O7	141.4 (3)	O4—Gd1—O3	50.0 (4)	Gd2—O7—Gd1^{ii}	109.7 (4)
O2—Gd1—O7^{ii}	79.5 (4)	O4—Gd1—N1^{iii}	123.0 (4)	Gd2^{i}—O1—Gd1^{i}	93.3 (3)
O2—Gd1—O1^{iii}	118.0 (3)	O7^{iv}—Gd2—O7	120.1 (5)	Gd2^{i}—O8—Gd1^{ii}	96.8 (3)
O2—Gd1—O8^{ii}	74.9 (3)	O7—Gd2—O1^{iii}	70.8 (4)	Gd2—O8—Gd1^{ii}	108.6 (3)
O2—Gd1—O6	138.4 (4)	O7—Gd2—O1^{ii}	83.0 (3)	Gd2—O8—Gd2^{i}	109.2 (3)
O2—Gd1—O3	68.9 (4)	O7—Gd2—O8^{iv}	147.8 (4)		
Symmetry codes: (i) *y*, -*x*+1, *z*; (ii) *y*, *x*, -*z*+1; (iii) -*y*+1, *x*, *z*; (iv) -*x*+1, *y*, -*z*+1.					

Table S5. *SHAPE* analysis of the Gd1 ion in **1**.

Label	Shape	Symmetry	Distortion(°)
EP-9	D_{9h}	Enneagon	35.694
OPY-9	C_{8v}	Octagonal pyramid	21.181
HBPY-9	D_{7h}	Heptagonal bipyramid	15.653
JTC-9	C_{3v}	Johnson triangular cupola J3	14.849
JCCU-9	C_{4v}	Capped cube J8	6.577
CCU-9	C_{4v}	Spherical-relaxed capped cube	4.976
JCSAPR-9	C_{4v}	Capped square antiprism J10	4.043
CSAPR-9	C_{4v}	Spherical capped square antiprism	3.138
JTCTPR-9	D_{3h}	Tricapped trigonal prism J51	4.396
TCTPR-9	D_{3h}	Spherical tricapped trigonal prism	2.944
JTDIC-9	C_{3v}	Tridiminished icosahedron J63	10.716
HH-9	C_{2v}	Hula-hoop	9.657
MFF-9	C_{s}	Muffin	3.413

Table S6. *SHAPE* analysis of the Gd1 ion in **2**.

Label	Shape	Symmetry	Distortion(°)
EP-9	D_{9h}	Enneagon	32.591
OPY-9	C_{8v}	Octagonal pyramid	22.014
HBPY-9	D_{7h}	Heptagonal bipyramid	18.939
JTC-9	C_{3v}	Johnson triangular cupola J3	14.291
JCCU-9	C_{4v}	Capped cube J8	8.965
CCU-9	C_{4v}	Spherical-relaxed capped cube	8.510
JCSAPR-9	C_{4v}	Capped square antiprism J10	2.349
CSAPR-9	C_{4v}	Spherical capped square antiprism	1.506
JTCTPR-9	D_{3h}	Tricapped trigonal prism J51	2.368
TCTPR-9	D_{3h}	Spherical tricapped trigonal prism	2.024
JTDIC-9	C_{3v}	Tridiminished icosahedron J63	12.280
HH-9	C_{2v}	Hula-hoop	11.853
MFF-9	C_s	Muffin	1.744

Table S7. *SHAPE* analysis of the Gd2 ion for complex **2**.

Label	Shape	Symmetry	Distortion(°)
OP-8	D_{8h}	Octagon	29.776
HPY-8	C_{7v}	Heptagonal pyramid	24.000
HBPY-8	D_{6h}	Hexagonal bipyramid	15.894
CU-8	O_h	Cube	8.187
SAPR-8	D_{4d}	Square antiprism	0.299
TDD-8	D_{2d}	Triangular dodecahedron	2.200
JGBF-8	D_{2d}	Johnson gyrobifastigium J26	16.646
JETBPY-8	D_{3h}	Johnson elongated triangular bipyramid J14	29.555
JBTPR-8	C_{2v}	Biaugmented trigonal prism J50	3.126

BTPR-8	C_{2v}	Biaugmented trigonal prism	2.542
JSD-8	D_{2d}	Snub diphenoid J84	5.451
TT-8	T_d	Triakis tetrahedron	9.062
ETBPY-8	D_{3h}	Elongated trigonal bipyramid	24.615

Table S8. *SHAPE* analysis of the Gd3 ion in **2**.

Label	Shape	Symmetry	Distortion(°)
EP-9	D_{9h}	Enneagon	32.142
OPY-9	C_{8v}	Octagonal pyramid	22.093
HBPY-9	D_{7h}	Heptagonal bipyramid	18.167
JTC-9	C_{3v}	Johnson triangular cupola J3	14.591
JCCU-9	C_{4v}	Capped cube J8	7.976
CCU-9	C_{4v}	Spherical-relaxed capped cube	7.555
JCSAPR-9	C_{4v}	Capped square antiprism J10	2.420
CSAPR-9	C_{4v}	Spherical capped square antiprism	1.683
JTCTPR-9	D_{3h}	Tricapped trigonal prism J51	2.549
TCTPR-9	D_{3h}	Spherical tricapped trigonal prism	2.424
JTDIC-9	C_{3v}	Tridiminished icosahedron J63	11.614
HH-9	C_{2v}	Hula-hoop	10.669
MFF-9	C_s	Muffin	1.922

Table S9. *SHAPE* analysis of the Gd1 ion in **3**.

Label	Shape	Symmetry	Distortion(°)
EP-9	D_{9h}	Enneagon	32.708
OPY-9	C_{8v}	Octagonal pyramid	20.651
HBPY-9	D_{7h}	Heptagonal bipyramid	16.489
JTC-9	C_{3v}	Johnson triangular cupola J3	15.277
JCCU-9	C_{4v}	Capped cube J8	8.576

CCU-9	C_{4v}	Spherical-relaxed capped cube	7.386
JCSAPR-9	C_{4v}	Capped square antiprism J10	2.800
CSAPR-9	C_{4v}	Spherical capped square antiprism	1.813
JTCTPR-9	D_{3h}	Tricapped trigonal prism J51	3.501
TCTPR-9	D_{3h}	Spherical tricapped trigonal prism	3.038
JTDIC-9	C_{3v}	Tridiminished icosahedron J63	11.410
HH-9	C_{2v}	Hula-hoop	7.768
MFF-9	C_s	Muffin	1.794

Table S10. *SHAPE* analysis of the Gd2 ion for complex **3**.

Label	Shape	Symmetry	Distortion(°)
OP-8	D_{8h}	Octagon	25.308
HPY-8	C_{7v}	Heptagonal pyramid	23.572
HBPY-8	D_{6h}	Hexagonal bipyramid	15.473
CU-8	O_h	Cube	8.133
SAPR-8	D_{4d}	Square antiprism	0.763
TDD-8	D_{2d}	Triangular dodecahedron	2.286
JGBF-8	D_{2d}	Johnson gyrobifastigium J26	15.449
JETBPY-8	D_{3h}	Johnson elongated triangular bipyramid J14	26.890
JBTPR-8	C_{2v}	Biaugmented trigonal prism J50	3.069
BTPR-8	C_{2v}	Biaugmented trigonal prism	2.794
JSD-8	D_{2d}	Snub diphenoid J84	5.219
TT-8	T_d	Triakis tetrahedron	8.724
ETBPY-8	D_{3h}	Elongated trigonal bipyramid	21.303

Thermal analysis.

The thermal stability of all complexes were investigated at a heating rate of 5 °C/min over the temperature range from 30 to 1000 °C in flowing N_2. There was no weight loss before 275 °C for **1**.

At a temperature close to 300 °C, a large weight change occurred, there was a weight loss of 86.45% and the remaining 13.55%. The remaining 13.55% after high temperature may be Gd_2O_3 (*calc*. 14.11%) (Figure S1a). For complex **2**, the TG data showed that the weight loss was mainly composed of three stages: the first weightlessness of 3.63 % before 100 °C. The weightlessness process basically corresponds to two free CH_3OH and one free H_2O (*calc.* 2.67%). The second weightlessness process occurred in the temperature range 100 ~ 300 °C, losing 12.62% of the total mass. The weightlessness process basically corresponds to eight coordinated NO_3^- anions (*calc.* 13.14%). The last weightlessness process occurred in the temperature range 300 ~ 950 °C, losing 27.64% of the total mass. It can be attributed to the thermal decomposition of organic components and coordination solvent molecules, which is close to the measured value of 29.60%. The remaining 56.09% may be Gd_2O_3 (*calc.* 54.14%) (Figure S1b). For complex **3**, there was a weight loss of 17.49% before 150 °C, which was determined by analysis to be twenty two free CH_3OH (calc. 12.86%). The second weightlessness process occurred in the temperature range 120 ~ 400 °C, losing 31.76% of the total mass. This is due to the loss of twenty-five CH_3CN (calc. 31.60 %). The remaining 42.74% may be Gd_2O_3 (*calc.* 43.10%) (Figure S1c). The PXRD data are presented in Figure S2.

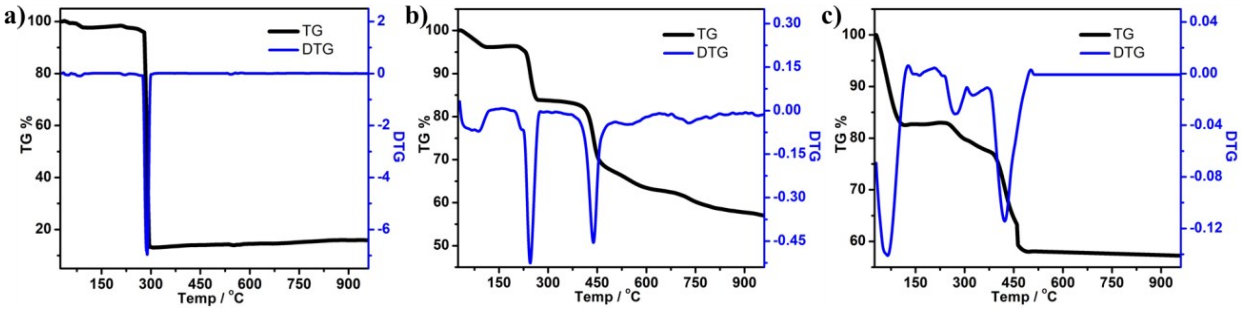

Figure S1. The TG curve of **1** (a), **2** (b) and **3** (c) under heating in flowing N_2 at 5 °C·min^{-1} over the temperature range of 35-1000 °C.

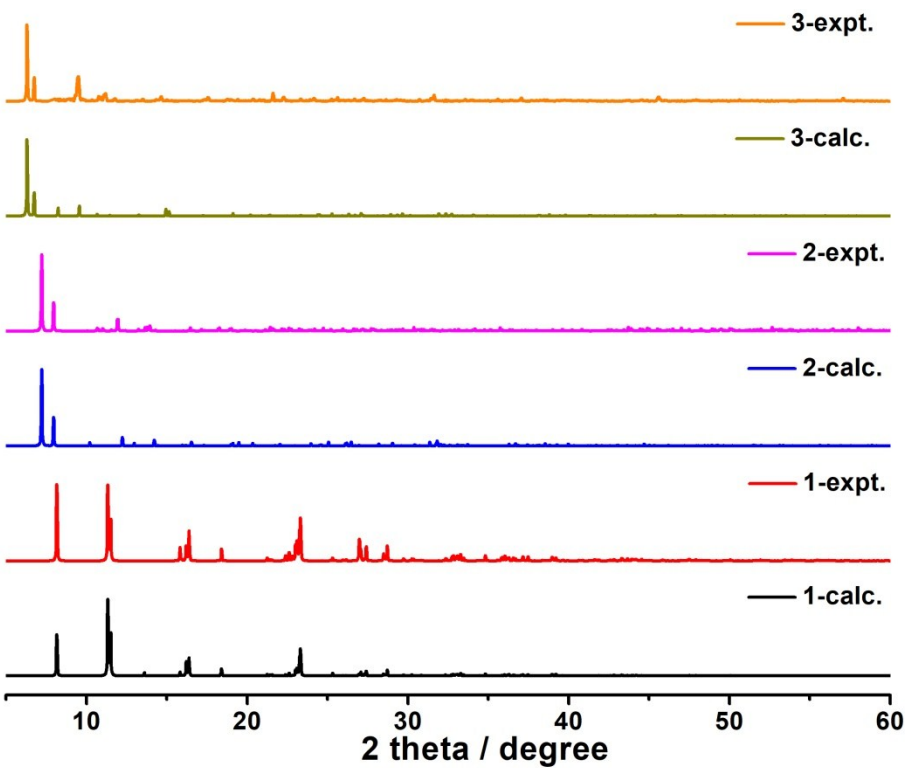

Figure S2. Powdered X-ray diffraction (PXRD) patterns for complexes **1**, **2** and **3**.

Table S11. Major species assigned in the Time-dependent HRESI-MS of **1** in positive mode.

m/z	Fragment	Relative Intensity									
		0min	10min	30min	1h	2h	3 h	6h	12	24h	48h
195.11	$[(H\mathbf{L^1})+H]^+$ (*calc.*195.11)	1	1	1	0.724	0.530	0.396	0.201	0.093	0.028	0
431.02	$[Gd(\mathbf{L^1})(NO_3)(H_2O)]^+$ (*calc.*431.02)	0.010	0.211	0.273	0.679	0.583	0.432	0.544	0.304	0.050	0.026
486.06	$[Gd(\mathbf{L^1})(NO_3)(H_2O)_4]^+$ (*calc.*486.06)	0.193	0.210	0.128	0.242	0.303	0.223	0.170	0.074	0.006	0
503.06	$[Gd(\mathbf{L^1})(NO_3)(H_2O)_5]^+$ (*calc.*503.06)	0.025	0.385	0.704	1	1	1	0.803	0.484	0.201	0.070
517.08	$[Gd(\mathbf{L^1})(NO_3)(H_2O)_4(CH_3OH)]^+$ (*calc.*517.08)	0.195	0.209	0.118	0.210	0.345	0.226	0.151	0.061	0.004	0
559.12	$[Gd(\mathbf{L^1})(NO_3)(CH_3OH)_2(CH_3CN)_2]^+$ (*calc.*559.12)	0.001	0.066	0.046	0.057	0.088	0.080	0.048	0.015	0.002	0
574.12	$[Gd(\mathbf{L^1})_2(CH_2O)]^+$ (*calc.*574.13)	0	0.053	0.112	0.102	0.131	0.154	0.098	0.041	0.044	0.014
756.90	$[Gd_2(\mathbf{L^1})(NO_3)_4]^+$ (*calc.*756.90)	0	0.009	0.012	0.051	0.144	0.194	0.110	0.097	0.135	0.208
798.97	$[Gd_2(\mathbf{L^1})(NO_3)_3(CH_3O)(CH_3OH)(CH_3CN)]^+$ (*calc.*799.00)	0.022	0.083	0.052	0.237	0.440	0.561	1	0.875	0.569	0.795
814.00	$[Gd_2(\mathbf{L^1})(NO_3)_3(CH_3O)(H_2O)_5]^+$ (*calc.*814.00)	0	0.042	0.091	0.196	0.302	0.605	0.509	0.445	1	0.912
829.96	$[Gd_2(\mathbf{L^1})(NO_3)_4(CH_3OH)(CH_3CN)]^+$ (*calc.*829.95)	0	0.029	0.050	0.101	0.314	0.601	0.321	0.278	0.541	0.222
857.05	$[Gd_2(\mathbf{L^1})_2(NO_3)_2(CH_3O)]^+$ (*calc.*857.04)	0.008	0.030	0.032	0.055	0.077	0.151	0.362	0.397	0.350	0.507
873.03	$[Gd_2(\mathbf{L^1})_2(NO_3)_2(CH_3O)(H_2O)]^+$ (*calc.*873.04)	0.031	0.068	0.055	0.125	0.260	0.519	0.834	0.915	0.613	0.577
888.02	$[Gd_2(\mathbf{L^1})_2(NO_3)_3]^+$ (*calc.*888.01)	0.081	0.076	0.082	0.142	0.566	0.711	0.918	1	0.893	1
917.99	$[Gd2(\mathbf{L^1})_2(NO_3)_3(CH_2O)]^+$ (*calc.*918.00)	0	0.004	0.043	0.027	0.061	0.285	0.053	0.057	0.469	0.111

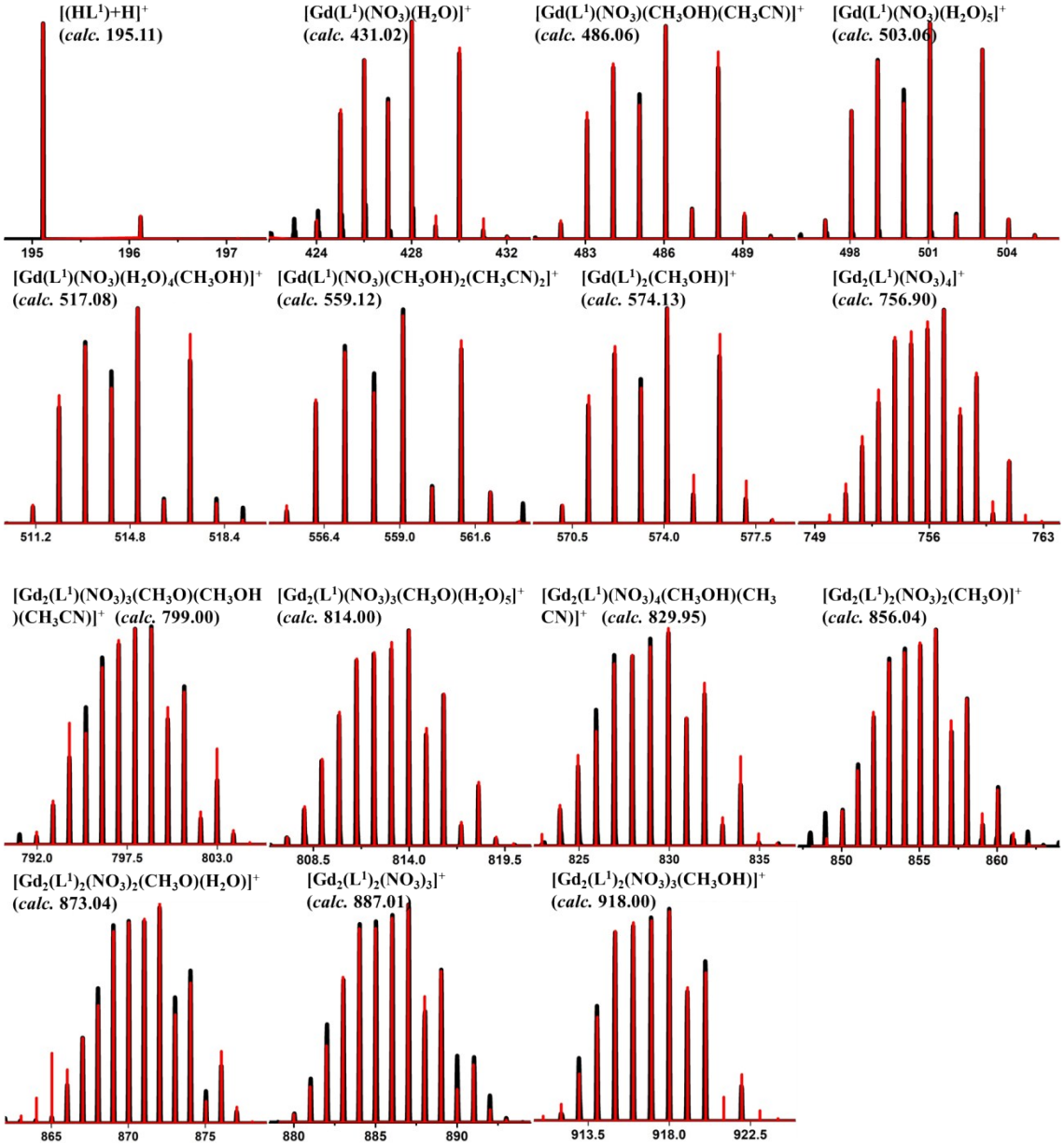

Figure S3a. The superposed simulated and observed spectra of several species in the Time-dependent HRESI-MS of **1**.

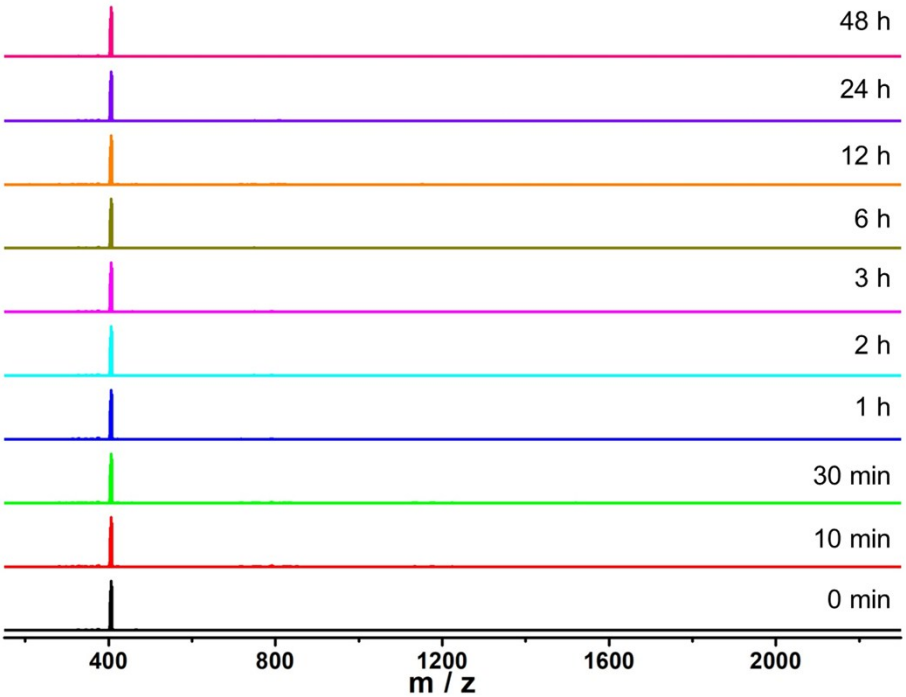

Figure S3b. Time-dependent HRESI-MS spectra for stepwise assembly of **1** in a negative mode.

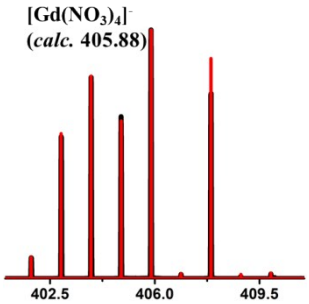

Figure S3c. The superposed simulated and observed spectra of several species in the time-dependent HRESI-MS of **1**.

Table S12. Major species assigned in the Time-dependent HRESI-MS of **2** in positivemode.

m/z	Fragment	Relative Intensity									
		0min	10min	30min	1h	2h	3 h	6h	12	24h	48h
106.09	$[(H\mathbf{L^2})+H]^+$ (*calc.*106.09)	1	1	0.697	0.663	0.516	0.307	0.256	0.118	0.078	0
366.06	$[Gd(\mathbf{L^2})(OH)(CH_3OH)(H_2O)_3H]^+$(*calc.*366.06)	0.027	0.058	0.941	0.480	0.693	0.180	0.076	0.017	0	0
470.09	$[Gd(\mathbf{L^2})(NO_3)(C_3H_7NO)_2]^+$(*calc.*470.09)	0.608	0.692	1	1	0.741	0.374	0.164	0	0	0
533.08	$[Gd(\mathbf{L^2})(NO_3)_2(C_3H_7NO)_2H]^+$(*calc.*533.08)	0	0.157	0.146	0.321	0.241	0.124	0.053	0	0	0
543.12	$[Gd(\mathbf{L^2})(NO_3)(C_3H_7NO)_3]^+$(*calc.*543.14)	0	0.395	0.690	0.849	0.629	0.317	0.141	0	0	0
709.95	$[Gd_2(\mathbf{L^2})_2(NO_3)_3]^+$(*calc.* 709.95)	0.048	0.241	0.607	0.346	0.274	0.227	0.140	0.039	0.024	0.027
751.03	$[Gd_2(\mathbf{L^2})_2(NO_3)_2(CH_3O)(H_2O)_4]^+$(*calc.*751.03)	0.003	0.016	0.212	0.244	0.124	0.025	0.013	0.003	0	0
782.00	$[Gd_2(\mathbf{L^2})_2(NO_3)_3(H_2O)_4]^+$(*calc.*782.00)	0	0.335	0.338	0.707	0.640	0.479	0.287	0.061	0.023	0.011
856.05	$[Gd_2(\mathbf{L^2})_2(NO_3)_3(C_3H_7NO)_2]^+$(*calc.*856.06)	0.007	0.326	0.107	0.865	1	0.683	0.384	0.057	0.013	0.003
1017.97	$[Gd_3(\mathbf{L^2})_3(NO_3)_3(CH_3O)(OH)]^+$(*calc.*1017.97)	0	0	0.020	0.015	0.026	0.016	0	0	0	0
1032.99	$[Gd_3(\mathbf{L^2})_3(NO_3)_3(CH_3O)_2]^+$(*calc.*1032.99)	0	0	0.023	0	0	0	0	0	0	0
1048.94	$[Gd_3(\mathbf{L^2})_3(NO_3)_4(OH)]^+$(*calc.*1048.94)	0	0	0.028	0.044	0.075	0.155	0.095	0	0	0
1063.96	$[Gd_3(\mathbf{L^2})_3(NO_3)_4(CH_3O)]^+$(*calc.*1063.96)	0	0	0.036	0.046	0.055	0	0	0	0	0
1093.92	$[Gd_3(\mathbf{L^2})_3(NO_3)_5]^+$(*calc.*1093.90)	0.047	0.012	0.272	0.523	0.764	1	0.694	0.289	0.118	0.022
1136.02	$[Gd_3(\mathbf{L^2})_4(NO_3)_4]^+$(*calc.*1136.01)	0	0	0.081	0.447	0.520	0.110	0.047	0	0	0
1153.95	$[Gd_3(\mathbf{L^2})_3(NO_3)_5(CH_3CN)(H_2O)H]^+$(*calc.*1153.97)	0	0	0.068	0.044	0.075	0	0	0.010	0.033	0
1370.92	$[Gd_4(\mathbf{L^2})_4(NO_3)_5(O)]^+$(*calc.*1370.90)	0	0	0.063	0.216	0.531	0.646	1	0.530	0.125	0.079
1479.91	$[Gd_5(\mathbf{L^2})_4(NO_3)_2(OH)_6(O)(H_2O)_2]^+$(*calc.*1479.91)	0	0	0．002	0.003	0.215	0.376	0.773	1	0.657	0.495
1563.08	$[Gd_5(\mathbf{L^2})_4(O)(OH)_6(CH_3O)_2(C_3H_7NO)_2(CH_3OH)]^+$(*calc.*1563.09)	0	0	0.002	0.010	0.332	0	0	0	0	0
2872.79	$[Gd_9(\mathbf{L^2})_7(OH)_{10}(NO_3)_8(CH_3O)(CH_3OH)]^+$(*calc.*2872.79)	0	0	0	0	0.008	0.019	0.028	0.126	0.325	0.314

2915.80	$[Gd_9(\mathbf{L^2})_8(OH)_{10}(NO_3)_8]^+$(*calc.*2915.82)	0	0	0	0	0.061	0.135	0.165	0.580	1	1

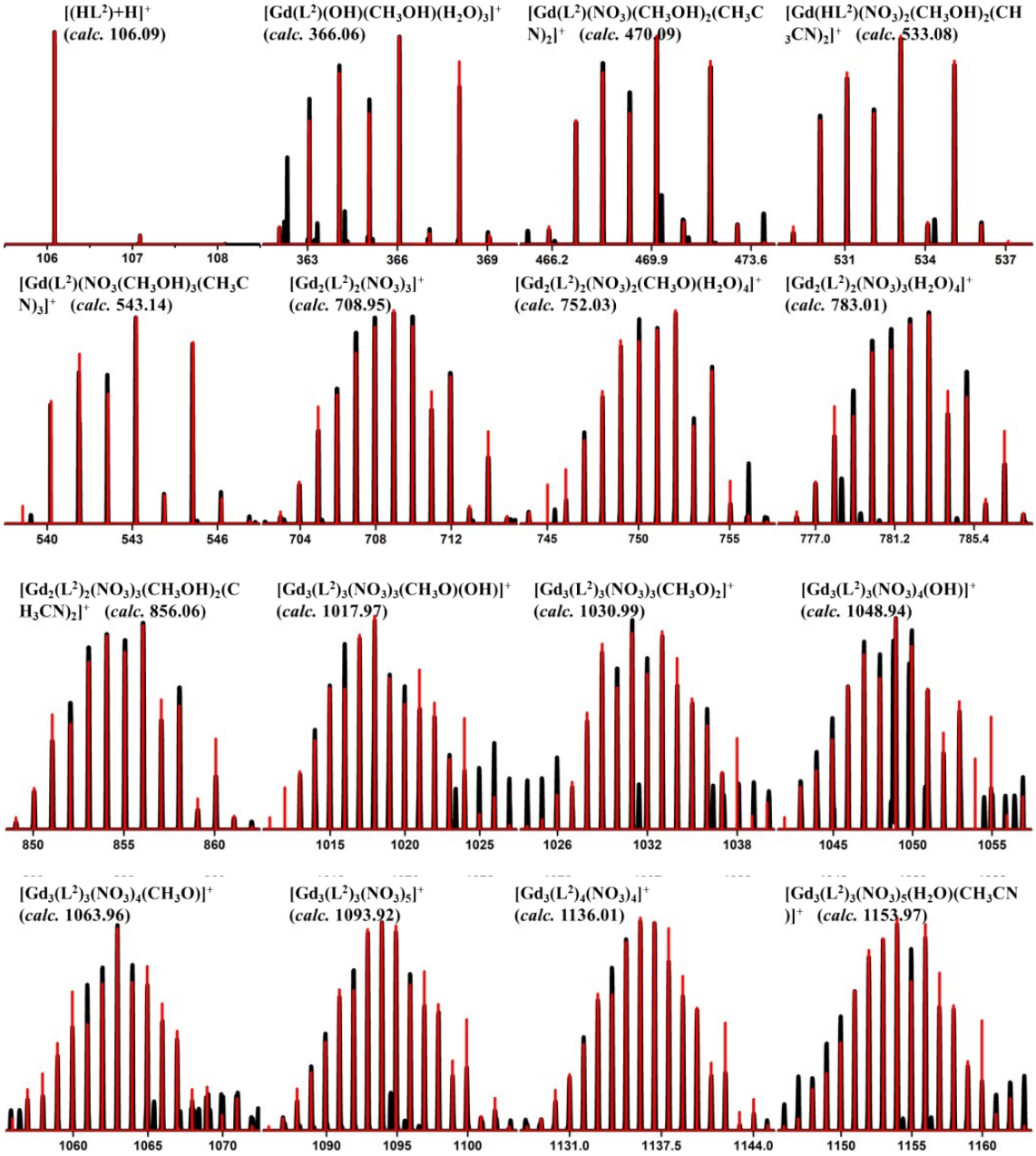
[(HL²)+H]⁺ (calc. 106.09)
[Gd(L²)(OH)(CH₃OH)(H₂O)₃]⁺ (calc. 366.06)
[Gd(L²)(NO₃)(CH₃OH)₂(CH₃CN)₂]⁺ (calc. 470.09)
[Gd(HL²)(NO₃)₂(CH₃OH)₂(CH₃CN)₂]⁺ (calc. 533.08)
[Gd(L²)(NO₃(CH₃OH)₃(CH₃CN)₃]⁺ (calc. 543.14)
[Gd₂(L²)₂(NO₃)₃]⁺ (calc. 708.95)
[Gd₂(L²)₂(NO₃)₂(CH₃O)(H₂O)₄]⁺ (calc. 752.03)
[Gd₂(L²)₂(NO₃)₃(H₂O)₄]⁺ (calc. 783.01)
[Gd₂(L²)₂(NO₃)₃(CH₃OH)₂(CH₃CN)₂]⁺ (calc. 856.06)
[Gd₃(L²)₃(NO₃)₃(CH₃O)(OH)]⁺ (calc. 1017.97)
[Gd₃(L²)₃(NO₃)₃(CH₃O)₂]⁺ (calc. 1030.99)
[Gd₃(L²)₃(NO₃)₄(OH)]⁺ (calc. 1048.94)
[Gd₃(L²)₃(NO₃)₄(CH₃O)]⁺ (calc. 1063.96)
[Gd₃(L²)₃(NO₃)₅]⁺ (calc. 1093.92)
[Gd₃(L²)₄(NO₃)₄]⁺ (calc. 1136.01)
[Gd₃(L²)₃(NO₃)₅(H₂O)(CH₃CN)]⁺ (calc. 1153.97)

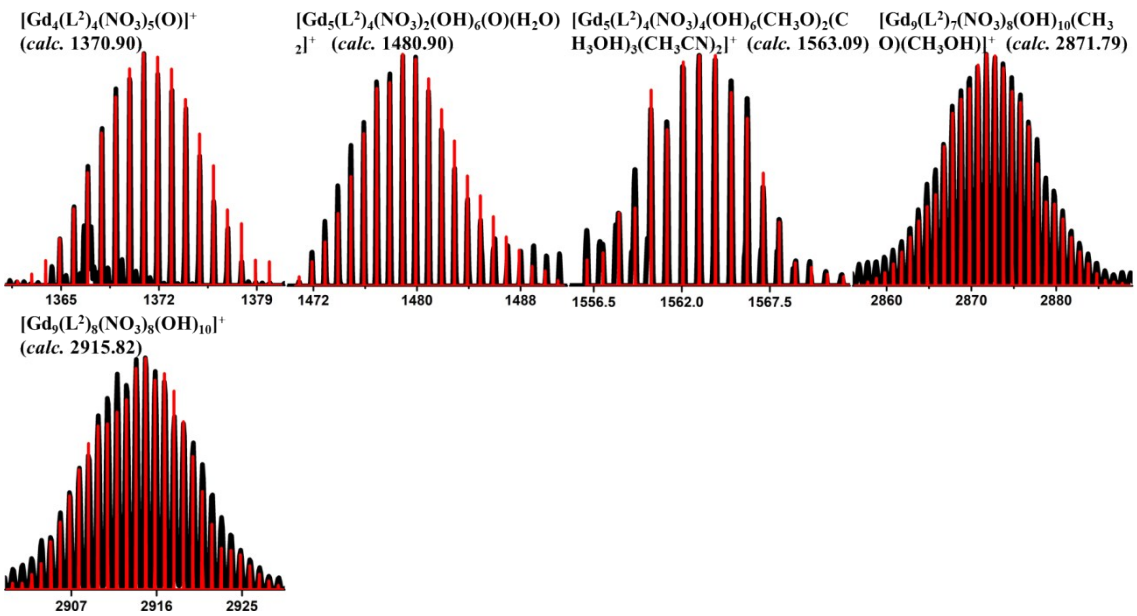

Figure S4a. The superposed simulated and observed spectra of several species in the time-dependent HRESI-MS of **2**.

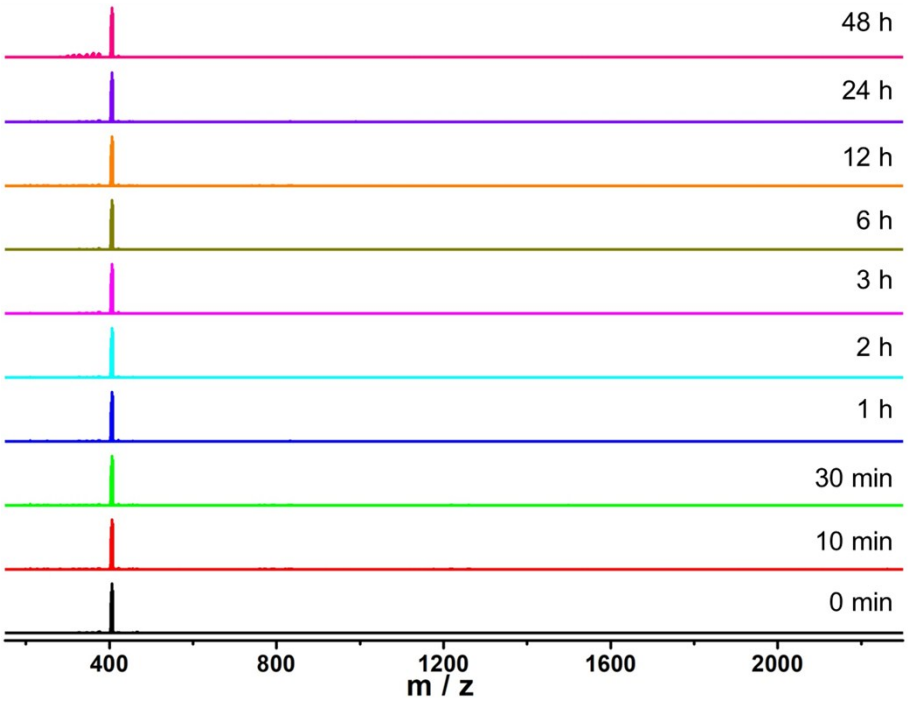

Figure S4b. Time-dependent HRESI-MS spectra for stepwise assembly of **2** in a negative mode.

Figure S4c. The superposed simulated and observed spectra of several species in the time-dependent HRESI-MS of **2**.

Table S13. Major species assigned in the Time-dependent HRESI-MS of **3** in positive mode.

m/z	Fragment	Relative Intensity									
		0min	10min	30min	1h	2h	3 h	6h	12	24h	48h
124.04	$[(\mathbf{L^3})H]^+$ (*calc.* 124.04)	1	1	0.903	0.817	0.761	0.599	0.476	0.328	0.140	0.051
328.98	$[Gd(\mathbf{L^3})(OH)(CH_3OH)]^+$ (*calc.* 328.98)	0.341	0.702	1	0.925	0.909	0.742	0.485	0.239	0.095	0.057
365.00	$[Gd(\mathbf{L^3})(OH)(CH_3OH)(H_2O)_2]^+$ (*calc.* 365.00)	0.286	0.597	0.982	0.959	1	0.827	0.649	0.322	0.183	0.086
391.98	$[Gd(\mathbf{L^3})(NO_3)(CH_3OH)(H_2O)]^+$ (*calc.* 391.97)	0.312	0.663	0.894	1	0.967	0.793	0.511	0.383	0.172	0.073
428.00	$[Gd(\mathbf{L^3})(NO_3)(H_2O)_3(CH_3OH)]^+$ (*calc.* 427.99)	0.193	0.523	0.832	0.954	0.918	0.907	0.756	0.386	0.112	0.041
442.01	$[Gd(\mathbf{L^3})(NO_3)(H_2O)_2(CH_3OH)_2]^+$ (*calc.* 442.01)	0.207	0.418	0.873	0.942	0.906	0.798	0.521	0.379	0.126	0.068
500.05	$[Gd(\mathbf{L^3})(NO_3)(CH_3OH)(H_2O)_7]^+$ (*calc.* 500.04)	0.136	0.351	0.575	0.726	0.805	0.702	0.538	0.329	0.173	0.082
754.96	$[Gd_2(\mathbf{L^3})_2(NO_3)(OH)_2(CH_3OH)_2(H_2O)_2]^+$ (*calc.* 754.96)	0	0	0.179	0.306	0.684	0.931	1	0.895	0.577	0.206
773.97	$[Gd_2(\mathbf{L^3})_2(NO_3)(OH)_2(H_2O)_3(CH_3OH)_2]^+$ (*calc.* 773.97)	0	0.023	0.206	0.567	0.835	1	0.976	0.707	0.422	0.193
803.94	$[Gd_2(\mathbf{L^3})_2(NO_3)_2(OH)(CH_3OH)(H_2O)_4]^+$ (*calc.* 803.94)	0.019	0.102	0.285	0.508	0.880	0.962	0.903	0.681	0.298	0.085
851.00	$[Gd_2(\mathbf{L^3})_2(NO_3)_2(CH_3O)(H_2O)_4(CH_3OH)_2]^+$ (*calc.* 850.99)	0.001	0.021	0.178	0.302	0.487	0.688	0.603	0.474	0.206	0.096
880.96	$[Gd_2(\mathbf{L^3})_2(NO_3)_3(CH_3OH)_2(H_2O)_4]^+$ (*calc.* 880.96)	0.012	0.121	0.205	0.388	0.473	0.363	0.408	0.265	0.094	0.022
938.98	$[Gd_2(\mathbf{L^3})_2(NO_3)_3(H_2O)_9(CH_3OH)]^+$ (*calc.* 939.00)	0.016	0.162	0.241	0.302	0.416	0.442	0.375	0.207	0.092	0.039
1012.04	$[Gd_2(\mathbf{L^3})_3(NO_3)_2(H_2O)_8(CH_3O)_2]$ (*calc.* 1012.02)	0.002	0.100	0.138	0.196	0.275	0.324	0.301	0.232	0.117	0.056
1265.96	$[Gd_3(\mathbf{L^3})_2(NO_3)_4(OH)_2(H_2O)_6(CH_3OH)_5]^+$ (*calc.* 1265.97)	0	0.048	0.114	0.153	0.202	0.231	0.183	0.268	0.116	0.103
1329.00	$[Gd_3(\mathbf{L^3})_2(NO_3)_4(OH)_2(H_2O)_6(CH_3OH)_7]^+$ (*calc.* 1329.02)	0	0.003	0.098	0.142	0.189	0.211	0.193	0.198	0.158	0.087
1342.01	$[Gd_3(\mathbf{L^3})_2(NO_3)_4(OH)_2(H_2O)_5(CH_3OH)_8]^+$ (*calc.* 1342.03)	0	0.003	0.084	0.122	0.163	0.182	0.166	0.171	0.136	0.075

1398.00	$[Gd_3(\mathbf{L^3})_2(NO_3)_5(OH)_2(H_2O)_8(CH_3OH)_6]^+$ (*calc.* 1398.02)	0	0.012	0.087	0.166	0.192	0.256	0.262	0.207	0.175	0.108
1458.05	$[Gd_3(\mathbf{L^3})_2(NO_3)_5(OH)(H_2O)_7(CH_3OH)_9]^+$ (*calc.* 1458.08)	0	0.009	0.064	0.105	0.167	0.199	0.231	0.190	0.100	0.043
1570.89	$[Gd_4(\mathbf{L^3})_4(NO_3)_3(OH)_4(H_2O)_4(CH_3OH)_4]^+$ (*calc.* 1570.90)	0	0	0.007	0.074	0.132	0.174	0.196	0.162	0.103	0.061
1633.91	$[Gd_4(\mathbf{L^3})_2(NO_3)_6(OH)_3(H_2O)_8(CH_3OH)_6]^+$ (*calc.* 1633.92)	0	0	0.009	0.096	0.149	0.193	0.211	0.173	0.124	0.089
1671.91	$[Gd_4(\mathbf{L^3})_2(NO_3)_7(OH)_2(H_2O)_4(CH_3OH)_8]^+$ (*calc.* 1671.93)	0	0.001	0.005	0.057	0.172	0.163	0.197	0.155	0.179	0.137
1731.83	$[Gd_5(\mathbf{L^3})_2(NO_3)_5(OH)_8(H_2O)_7(CH_3OH)_4]^+$ (*calc.* 1731.82)	0	0	0.003	0.051	0.126	0.168	0.182	0.215	0.196	0.228
1792.89	$[Gd_5(\mathbf{L^3})_2(NO_3)_5(OH)_7(H_2O)_6(CH_3OH)_7]^+$ (*calc.* 1792.89)	0	0	0.001	0.012	0.097	0.152	0.180	0.203	0.228	0.204
1909.70	$[Gd_{12}(\mathbf{L^3})_8(OH)_{16}(NO_3)_6(OH)_4(H_2O)_8(CH_3OH)_2]^{2+}$ (*calc.* 1909.71)	0	0	0	0.018	0.267	0.683	1	0.928	1	1
1942.25	$[Gd_{12}(\mathbf{L^3})_8(OH)_{16}(NO_3)_6(OH)_4(H_2O)_8(CH_3OH)_4]^{2+}$ (*calc.* 1942.24)	0	0	0	0.029	0.302	0.635	0.898	1	0.962	0.941
2053.75	$[Gd_{12}(\mathbf{L^3})_9(OH)_{16}(NO_3)_8(OH)(H_2O)_8(CH_3OH)_6]^{2+}$ (*calc.* 2053.74)	0	0	0	0.024	0.293	0.589	0.805	0.917	0.948	0.963
2135.76	$[Gd_6(\mathbf{L^3})_2(NO_3)_8(OH)_7(H_2O)_6(CH_3OH)_7]^+$ (*calc.* 2135.77)	0	0	0	0.004	0.017	0.058	0.095	0.118	0.136	0.178
2194.76	$[Gd_6(\mathbf{L^3})_2(NO_3)_8(OH)_7(H_2O)_{11}(CH_3OH)_6]^+$ (*calc.* 2194.79)	0	0	0	0.001	0.013	0.046	0.087	0.104	0.123	0.166
2255.81	$[Gd_6(\mathbf{L^3})_2(NO_3)_9(OH)_6(H_2O)_{12}(CH_3OH)_6]^+$ (*calc.* 2255.80)	0	0	0	0.002	0.014	0.047	0.079	0.110	0.127	0.147

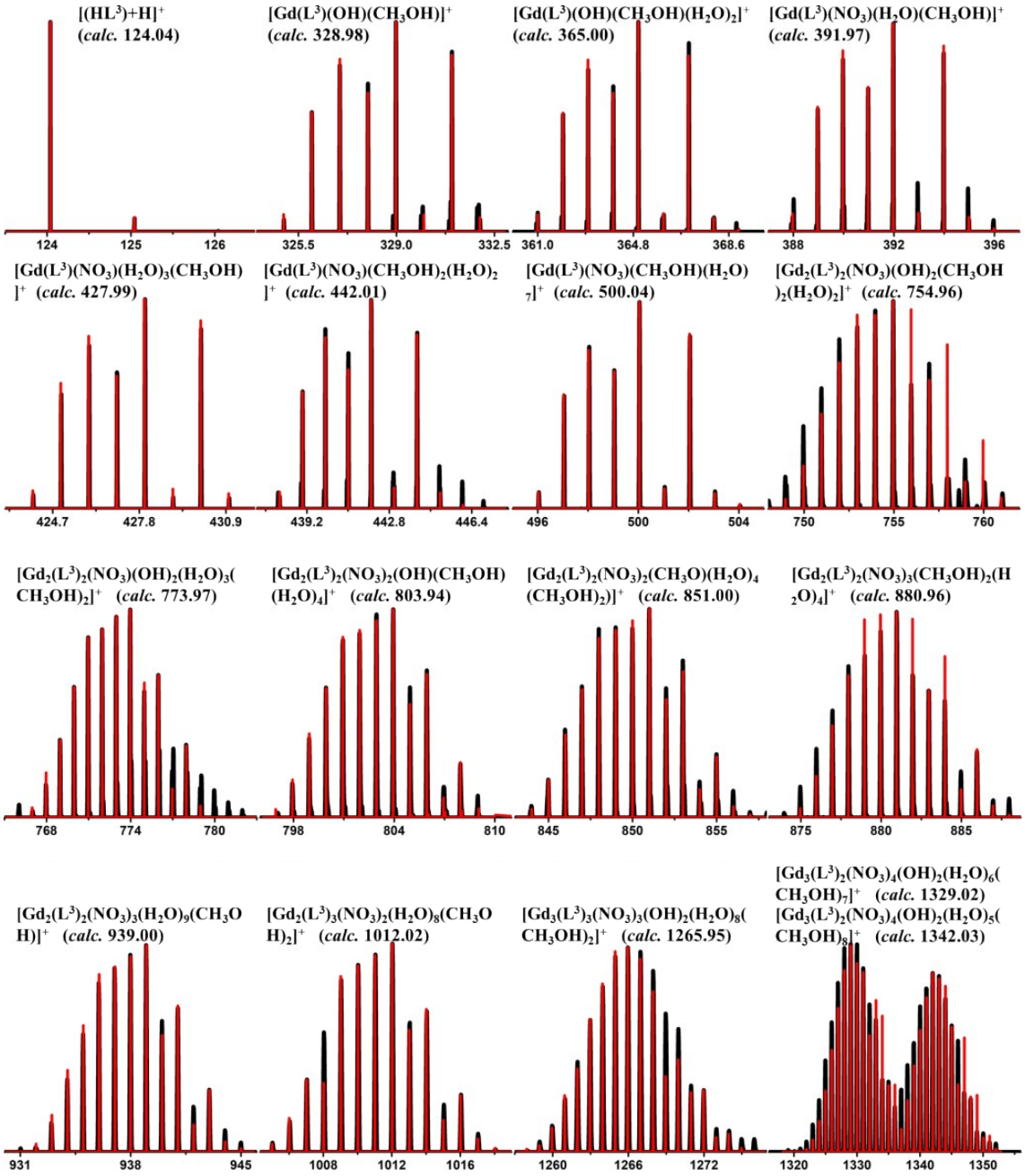
[(HL3)+H]+ (calc. 124.04)
[Gd(L3)(OH)(CH3OH)]+ (calc. 328.98)
[Gd(L3)(OH)(CH3OH)(H2O)2]+ (calc. 365.00)
[Gd(L3)(NO3)(H2O)(CH3OH)]+ (calc. 391.97)
[Gd(L3)(NO3)(H2O)3(CH3OH)]+ (calc. 427.99)
[Gd(L3)(NO3)(CH3OH)2(H2O)2]+ (calc. 442.01)
[Gd(L3)(NO3)(CH3OH)(H2O)7]+ (calc. 500.04)
[Gd2(L3)2(NO3)(OH)2(CH3OH)2(H2O)2]+ (calc. 754.96)
[Gd2(L3)2(NO3)(OH)2(H2O)3(CH3OH)2]+ (calc. 773.97)
[Gd2(L3)2(NO3)2(OH)(CH3OH)(H2O)4]+ (calc. 803.94)
[Gd2(L3)2(NO3)2(CH3O)(H2O)4(CH3OH)2)]+ (calc. 851.00)
[Gd2(L3)2(NO3)3(CH3OH)2(H2O)4]+ (calc. 880.96)
[Gd2(L3)2(NO3)3(H2O)9(CH3OH)]+ (calc. 939.00)
[Gd2(L3)3(NO3)2(H2O)8(CH3OH)2]+ (calc. 1012.02)
[Gd3(L3)3(NO3)3(OH)2(H2O)8(CH3OH)2]+ (calc. 1265.95)
[Gd3(L3)2(NO3)4(OH)2(H2O)6(CH3OH)7]+ (calc. 1329.02)
[Gd3(L3)2(NO3)4(OH)2(H2O)5(CH3OH)8]+ (calc. 1342.03)
124 125 126
325.5 329.0 332.5
361.0 364.8 368.6
388 392 396
424.7 427.8 430.9
439.2 442.8 446.4
496 500 504
750 755 760
768 774 780
798 804 810
845 850 855
875 880 885
931 938 945
1008 1012 1016
1260 1266 1272
1320 1330 1340 1350

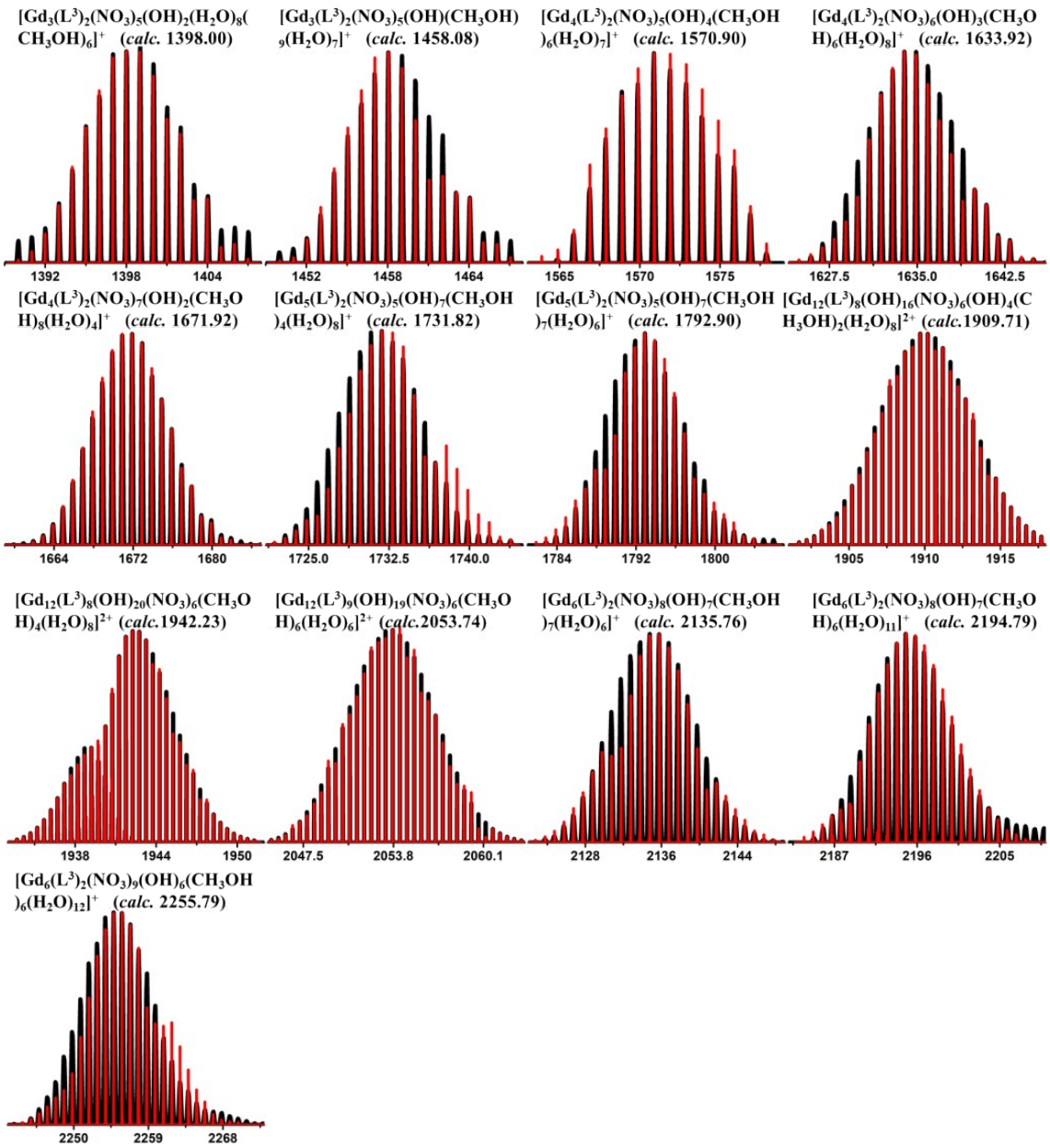

Figure S5a. The superposed simulated and observed spectra of several species in the time-dependent HRESI-MS of **3**.

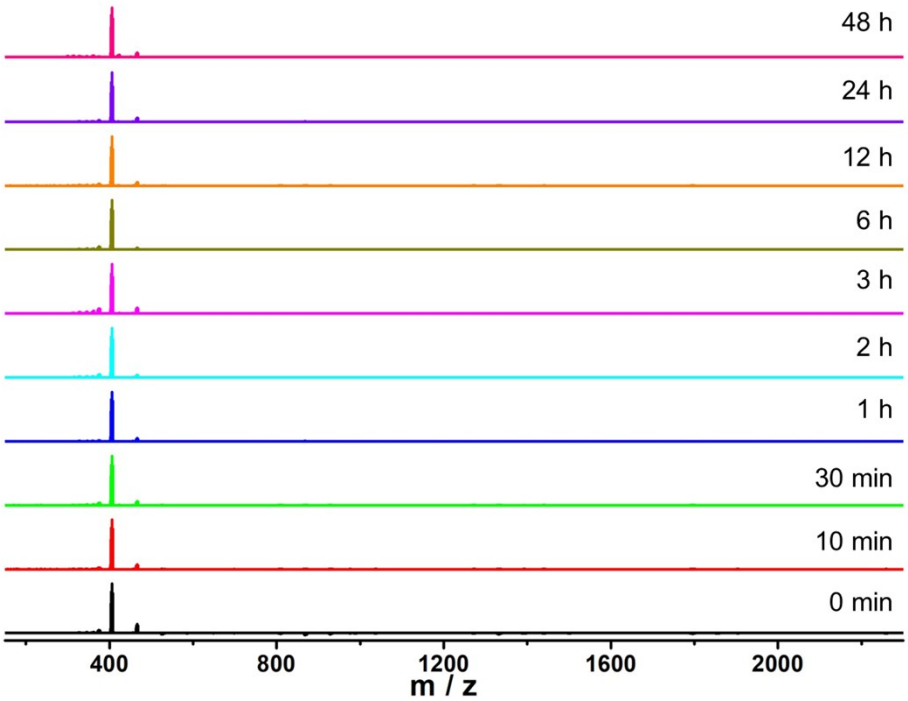

Figure S5b. Time-dependent HRESI-MS spectra for stepwise assembly of **3** in a positive mode.

Figure S5c. The superposed simulated and observed spectra of several species in the Time-dependent HRESI-MS of **3**.